AD-A183 076 AMBIENT SCATTERING FROM RING-SYMMETRIC SPACECRAFT EXHAUST PLUME(U) FALCOVITZ (JOSEPH) HAIFA (ISRAEL) J FALCOVITZ APR 87 NPS-72-87-003CR N00228-87-C-3046 1/1

UNCLASSIFIED F/G 20/4 NL

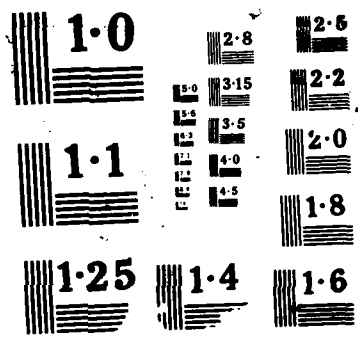
1.0
2.8
2.5
3.15
2.2
3.5
2.0
1.1
4.0
4.5
1.8
1.25
1.4
1.6

(2)

NPS72-87-003CR



# NAVAL POSTGRADUATE SCHOOL

## Monterey, California





CONTRACTOR REPORT

AMBIENT SCATTERING FROM RING-SYMMETRIC

SPACECRAFT EXHAUST PLUME

by

Joseph Falcovitz

April 1987

Approved for public release; distribution unlimited.

Prepared for: Strategic Defense Initiative Office
The Pentagon
Washington, DC 20301-7100

6

NAVAL POSTGRADUATE SCHOOL
Monterey, California

RADM R. C. Austin
Superintendent

D. A. Schrady
Provost

The work reported herein was performed for the Naval Postgraduate School by Dr. Joseph Falcovitz under contract N00228-87-C-3046. The work presented in this report is in support of "Rarefied Gas Dynamics of Laser Exhaust Plume" sponsored by the Strategic Defense Initiative Office/Directed Energy Office. This is the final report for that contract. The work provides information concerning scattering of exhaust molecules by ambient air and effects on spacecraft charging. The project at the Naval Postgraduate School is under the cognizance of Distinguished Professor A. E. Fuhs who is principal investigator.



Prepared by:

Joseph Falcovitz

DR. JOSEPH FALCOVITZ
Research Contractor

Reviewed by:

Allen E Fuhs

ALLEN E. FUHS
Distinguished Professor & Chairman
Space Systems Academic Group

Released by:

G E Schacher

G. E. SCHACHER
Dean of Science and Engineering

# REPORT DOCUMENTATION PAGE

| | |
|---|---|
| 1a. REPORT SECURITY CLASSIFICATION: UNCLASSIFIED | 1b. RESTRICTIVE MARKINGS: NONE  A183076 |
| 2a. SECURITY CLASSIFICATION AUTHORITY | 3. DISTRIBUTION/AVAILABILITY OF REPORT: Approved for Public Release; Distribution Unlimited |
| 2b. DECLASSIFICATION/DOWNGRADING SCHEDULE | |
| 4. PERFORMING ORGANIZATION REPORT NUMBER(S): NPS72-87-003CR | 5. MONITORING ORGANIZATION REPORT NUMBER(S): NPS72-87-003CR |
| 6a. NAME OF PERFORMING ORGANIZATION: JOSEPH FALCOVITZ / 6b. OFFICE SYMBOL (If applicable): Code 72 | 7a. NAME OF MONITORING ORGANIZATION: NAVAL POSTGRADUATE SCHOOL, CODE 72 |
| 6c. ADDRESS (City, State, and ZIP Code): Research Contractor, Naval Postgraduate School, Monterey, CA 93943-5100 | 7b. ADDRESS (City, State, and ZIP Code): Space Systems Academic Group, Monterey, CA 93943-5100 |
| 8a. NAME OF FUNDING/SPONSORING ORGANIZATION: Strategic Defense Initiative Office / 8b. OFFICE SYMBOL (If applicable): SDIO/DEO | 9. PROCUREMENT INSTRUMENT IDENTIFICATION NUMBER |
| 8c. ADDRESS (City, State, and ZIP Code): SDIO/DEO, Washington, DC 20301-7100 | 10. SOURCE OF FUNDING NUMBERS: PROGRAM ELEMENT NO. / PROJECT NO. / TASK NO. / WORK UNIT ACCESSION NO. |

11. TITLE (Include Security Classification): AMBIENT SCATTERING FROM RING-SYMMETRIC SPACECRAFT EXHAUST PLUME

12. PERSONAL AUTHOR(S): JOSEPH FALCOVITZ

| 13a. TYPE OF REPORT | 13b. TIME COVERED | 14. DATE OF REPORT (Year, Month, Day) | 15. PAGE COUNT |
|---|---|---|---|
| Contractor Report | FROM JAN 87 TO MAR 87 | April 1987 | 60 |

16. SUPPLEMENTARY NOTATION

| 17. COSATI CODES | | | 18. SUBJECT TERMS (Continue on reverse if necessary and identify by block number) |
|---|---|---|---|
| FIELD | GROUP | SUB-GROUP | Spacecraft Contamination, Exhaust Plume, Ambient Scattering, First Collision |

19. ABSTRACT (Continue on reverse if necessary and identify by block number)

We present a first-collision model for the evaluation of return flux from the exhaust plume of a ring-symmetric HF/DF laser in LEO, generated by an incident flux of ambient molecules traveling at orbital speed. The steady plume is bounded by a pair of lip-centered rarefaction fans, and unless spacecraft attitude enables incident air molecules to reach the plume through the cavitation regions that extend beyond these fans, the spacecraft is shielded from ambient scattering by its own plume. Assuming hard-spheres collisions, the first-collision model is given by a simple closed-form expression that can be regarded as a source term for scattered exhaust molecules. This source term is integrated numerically throughout the fan, yielding the flux arriving at some surface "target point". Quantitatively, it is shown that for a typical HF DF laser exhaust the contamination level generated by ambient scattering is not significant. It was found that the maximum return flux of HF−DF constitutes about 2% of the incident ambient flux; this ratio will be nearly constant for LEO altitudes. The value of this flux ratio is shown to be dependent on the molecular collision model; it may change upon replacing the hard-spheres approximation by a more realistic collision model. A possible modification of spacecraft charging by the exhaust was examined, including production of $HF^-$ and $DF^-$. The only significant effect seemed to be shadowing of the downstream half of the spacecraft at oblique orbital attitudes.

| | |
|---|---|
| 20. DISTRIBUTION/AVAILABILITY OF ABSTRACT: ☒ UNCLASSIFIED/UNLIMITED ☐ SAME AS RPT ☐ DTIC USERS | 21. ABSTRACT SECURITY CLASSIFICATION: UNCLASSIFIED |
| 22a. NAME OF RESPONSIBLE INDIVIDUAL: ALLEN E. FUHS, Distinguished Professor | 22b. TELEPHONE (Include Area Code): (408) 646-2948 / 22c. OFFICE SYMBOL: Code 72 |

DD FORM 1473, 84 MAR — 83 APR edition may be used until exhausted. All other editions are obsolete.

SECURITY CLASSIFICATION OF THIS PAGE

U.S. Government Printing Office: 1986—606-24

## ABSTRACT

We present a first-collision model for the evaluation of return flux from the exhaust plume of a ring-symmetric HF/DF laser in LEO, generated by an incident flux of ambient molecules traveling at orbital speed. The steady plume is bounded by a pair of lip-centered rarefaction fans, and unless spacecraft attitude enables incident air molecules to reach the plume through the cavitation regions that extend beyond these fans, the spacecraft is shielded from ambient scattering by its own plume. Assuming hard-spheres collisions, the first-collision model is given by a simple closed-form expression that can be regarded as a source term for scattered exhaust molecules. This source term is integrated numerically throughout the fan, yielding the flux arriving at some surface "target point". Quantitatively, it is shown that for a typical HF/DF laser exhaust the contamination level generated by ambient scattering is not significant. It was found that the maximum return flux of HF+DF constitutes about 2% of the incident ambient flux; this ratio will be nearly constant for LEO altitudes. The value of this flux ratio is shown to be dependent on the molecular collision model; it may change upon replacing the hard-spheres approximation by a more realistic collision model. A possible modification of spacecraft charging by the exhaust was examined, including production of $\mathbf{HF^-}$ and $\mathbf{DF^-}$. The only significant effect seemed to be shadowing of the downstream half of the spacecraft at oblique orbital attitudes.

## ACKNOWLEDGEMENTS

This work is part of a study involving gas dynamics of exhaust plumes from spacecrafts. It was conducted under the cognizance of Distinguished Professor Allen E. Fuhs, who initiated this research program at the Naval Postgraduate School. I wish to thank Professor Fuhs for his inspiring guidance and deeply appreciate his continued support.

## TABLE OF CONTENTS



## LIST OF FIGURES

## LIST OF TABLES

EMPTY PAGE

# 1. INTRODUCTION

This presentation is part of a study on the gas dynamics of ring-symmetric exhaust plumes in space, conducted at the Naval Postgraduate School in Monterey. A ring-symmetric jet has zero thrust, which makes it suitable as an exhaust configuration for various open loop power plants designed to produce high power for relatively short durations. One such system is an envisioned space-based chemical laser, shown schematically in Fig. 1-1. In the case of a chemical laser, a ring-symmetric configuration would also enable the laser radiation to emerge in the form of an axisymmetric beam.

The exhaust nozzle should be designed to bring the outgoing flow to a supersonic speed at the nozzle exit surface. The near field of a free jet is then composed of an inner core bounded by a pair of ring-symmetric rarefaction fans centered at the nozzle lips (Fig. 1-1). Beyond the limiting characteristic surface of the centered rarefaction waves (CRW), a near-vacuum condition prevails. For the purpose of continuum gas dynamic analysis, we assume it is a perfect vacuum.

An earth orbiting vehicle is subject to an oncoming stream of ambient molecules at a speed of $U_A \approx 8$ (km/sec), in a direction depending upon its orientation relative to the orbital velocity vector. This speed is sufficiently high to cause backscattering of exhaust molecules (see schematic description in Fig. 1-2) moving at speeds appropriate to chemical combustion (about 2 to 4 km/s). However, large exhaust plumes, having achieved stationary flow, may be sufficiently dense at their outer fringes to effectively trap and entrain all oncoming ambient molecules. Thus, ambient scattering may be significant only in selected ranges of attitude angles, at which ambient molecules can reach the vicinity of the spacecraft by traveling almost collisionlessly through cavitation regions. Exhaust molecules that may be "candidates" for ambient scattering will hence come from plume segments flanked by cavitation regions. The contribution of ambient scattering to contamination will thus be highly dependent upon spacecraft geometry and orientation. This may well affect spacecraft design and operating procedures.

The purpose of this report is to present a first-collision model for estimating the flux of exhaust molecules backscattered from the fringes of the plume by ambient molecules, along with results of sample flux computations performed on a typical HF/DF laser exhaust configuration. The flow field throughout the plume is assumed to be governed by the equations of continuum gas dynamics. In principle, the flow could be obtained by solving the governing equations, i.e., the equations for stationary isentropic flow in two-dimensional axisymmetric coordinates. In practice, this is normally accomplished by integrating the flow equations in characteristic form, using some finite difference scheme (method-of-characteristics). We have performed such computations, but given the complexity of applying them to the subsequent integration of ambient scattering flux (due to the need for two-dimensional interpolations from an irregular solution grid), we opted for a different alternative : a closed-form approximation to the ring-symmetric CRW, based on an analytic expression for flow variables along characteristic lines that fan out from the nozzle lip.

The plan of this report is as follows. In Ch. 2 we outline the approximation to the ring-symmetric CRW and present some computation results that demonstrate its accuracy. In Ch. 3 we describe the first-collision model and the 3-D spatial integration scheme for computing the flux arriving at the cylindrical spacecraft. In Ch. 4 some results of backscattered flux of corrosive molecules (HF + DF), showing flux variation with target point location ($X_s$) and attitude angles ($\psi_A$, $\varphi_A$) are presented. In Ch. 5 we take up the subject of spacecraft charging, using results of ambient scattering to assess the effect of laser exhaust on spacecraft charging. This is followed by concluding remarks in Ch. 6 and a list of references in Ch. 7. A concise description of the flux computation code "AMB" is given in Appendix A, followed by the code listing.

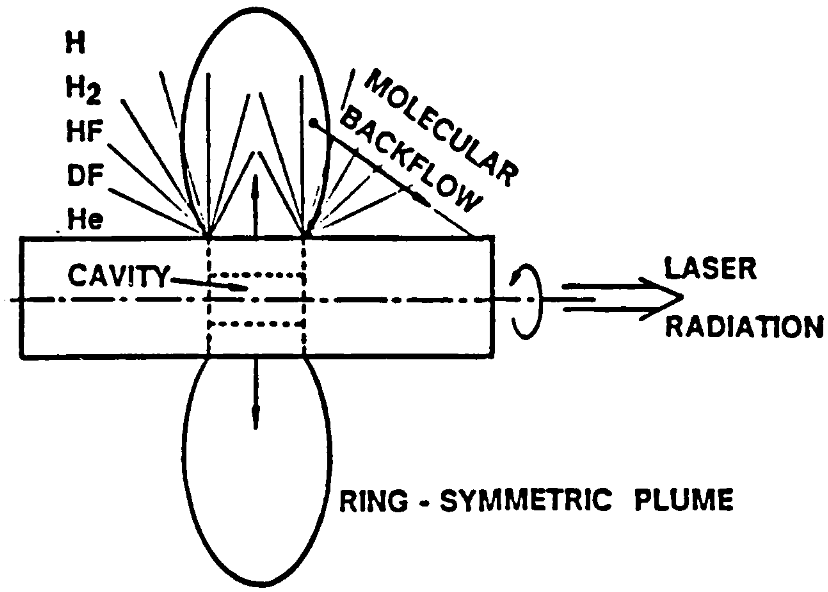


Figure 1-1. Ring-Symmetric HF/DF Laser Exhaust Plume.

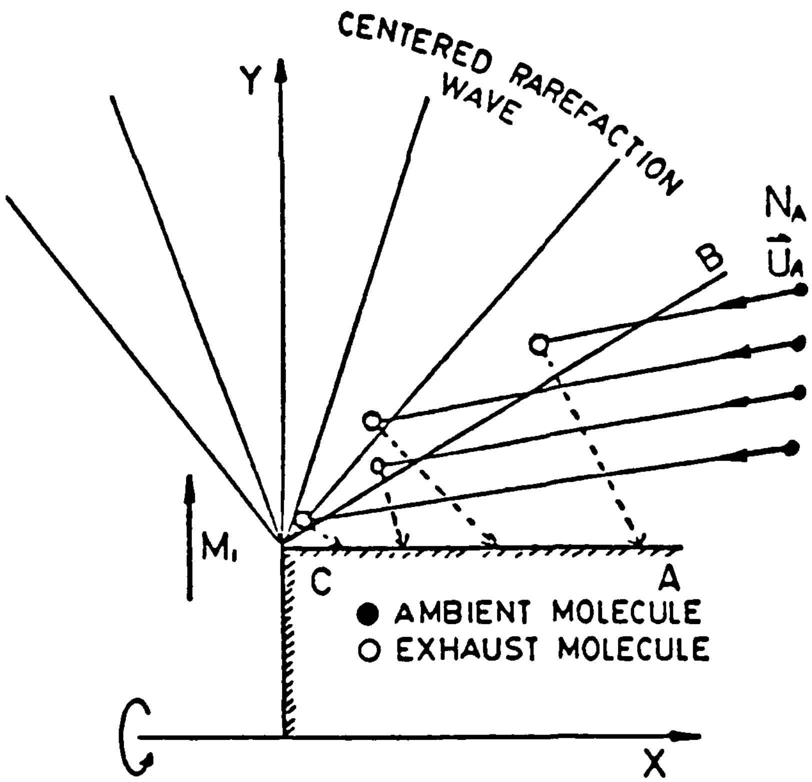


Figure 1-2. Schematic Description of Ambient Scattering. The Cavitation Region is Bounded by Lines CA and CB.

## 2. COMPUTATION OF THE PLUME FLOW FIELD

Most ambient molecules entering the CRW that flanks the exhaust plume are stopped within several mean free paths from their point of entry. A quantitative estimate of ambient back-scattering would thus depend on the flow field at the outer (hypersonic) fringes of the lip-centered CRW. Even though the flow in those regions is generally past the surface of continuum breakdown, the density there is reasonably well approximated by the continuum flow field, as demonstrated by Bird's Monte-Carlo simulation of a Prandtl-Meyer expansion to vacuum [1]. The evaluation of ambient scattering thus calls for an ancillary computational procedure capable of rendering the continuum flow field at a large number of points in the ring-symmetric CRW of an exhaust plume. This method was described in a recent report [2]. Here we just outline the key ideas and main results of this approximation method.

Our analytic approximation to a ring-symmetric CRW is formulated as follows. In a planar CRW (Prandtl-Meyer flow) all flow variables are uniform along the characteristic lines that fan out from the corner (we assume they are the $C^+$ family). In the ring-symmetric case the flow near the corner approaches asymptotically a corresponding planar CRW flow, which we term the *associate* CRW. However, the gradients along $C^+$ characteristics at the corner of a ring-symmetric CRW do not vanish as in a planar CRW. The key idea is thus : evaluate flow gradients in $C^+$ directions at the corner, then use them to extrapolate the associate CRW along $C^+$ lines to a finite distance from the corner. The extrapolation is a nonlinear function of the radial coordinate $y$, chosen so that the ensuing expression conforms exactly to the flow at the leading (exit) characteristic $C^+(\beta_l)$. Omitting all details of the analysis, the resulting approximation is presented as the following power-law :

$$f(\alpha,\beta) = f(0,\beta)\left[y(\alpha,\beta)/y(0,\beta)\right]^{\delta(0,\beta)} \qquad (2\text{-}1)$$

where $f$ is the streamtube area ratio for isentropic flows ( $f=1$ at a sonic point), $\beta$ is the Mach number of a particular characteristic line at the corner, $\alpha$ is a coordinate along the $C^+(\beta)$ characteristic line ( $\alpha=0$ at the corner), and $y$ is the radial coordinate of a point on the characteristic line $C^+(\beta)$. The Mach number at point $(\alpha,\beta)$ is readily determined from $f(\alpha,\beta)$ using the standard relation between area ratio and Mach number [3]. A closed-form expression for $\delta(0,\beta)$ was developed but is not given here; instead, this function is shown in Fig. 2-1. We note that $\delta$ approaches the asymptotic value of $2/(3-\gamma)$ as $\beta$ increases to infinity, and that generally $1 < \delta(0,\beta) < 2$ so that streamtubes diverge at a rate intermediate between that of cylindrical and spherical expansion flows.

Clearly, in an isentropic flow all thermodynamic variables, and in particular density, can be evaluated from **f**. This approximation is readily applied to the hypersonic portions of a ring-symmetric CRW since it turns out that characteristic lines are nearly straight there, which means that the characteristic line $C^{+}(\beta)$ passing through a given point can be readily determined. As a demonstration of the degree of accuracy obtainable from this approximation, we show in Fig. 2-2 the variation of Mach number along a characteristic line in the ring-symmetric CRW, compared with an accurate method-of-characteristics computation. This comparison demonstrates that the analytic approximation is reasonably accurate to nearly ten corner-radii away from the corner.

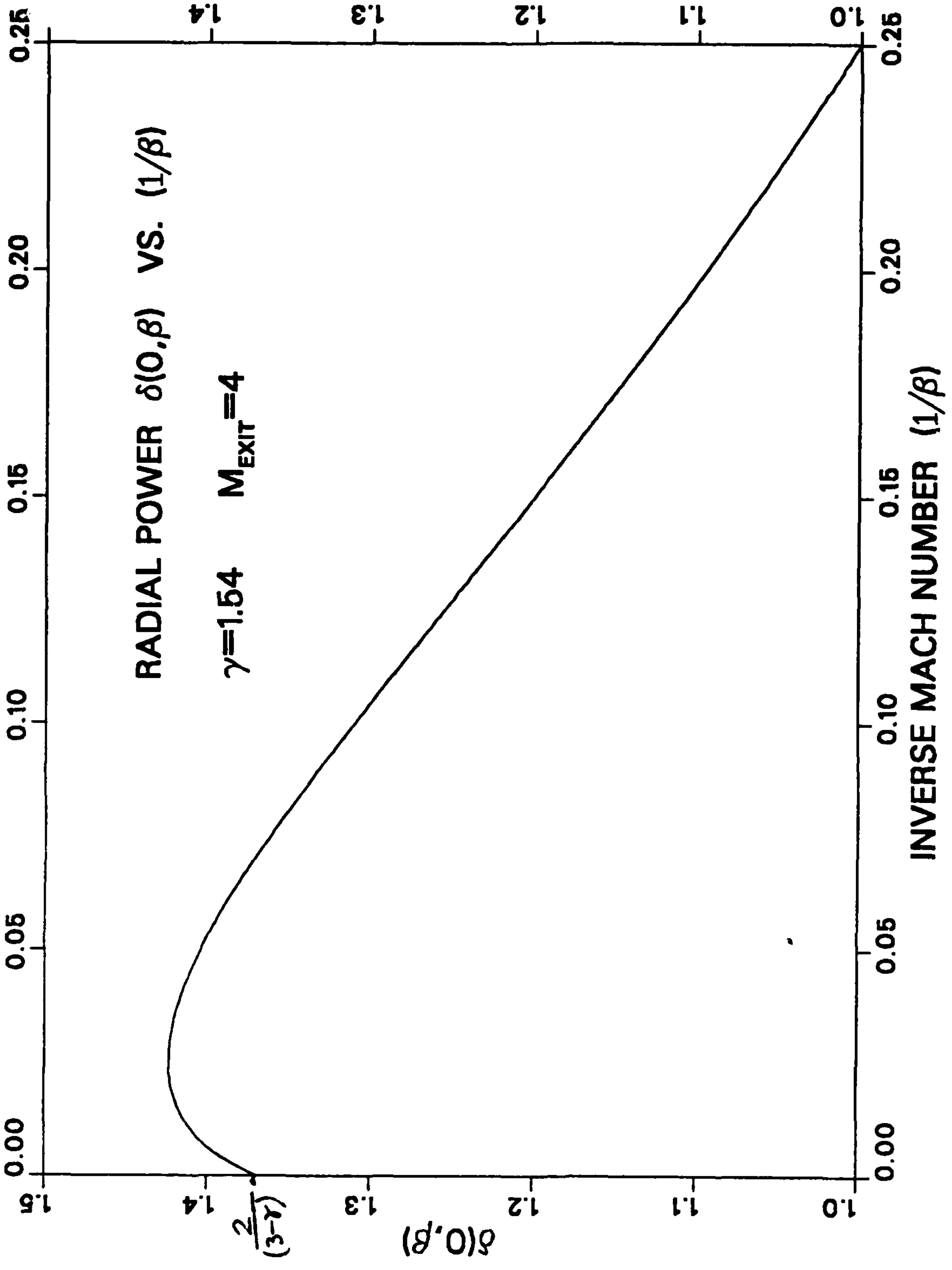


Figure 2-1. Power $\delta(0,\beta)$ for the power-law Approximation.

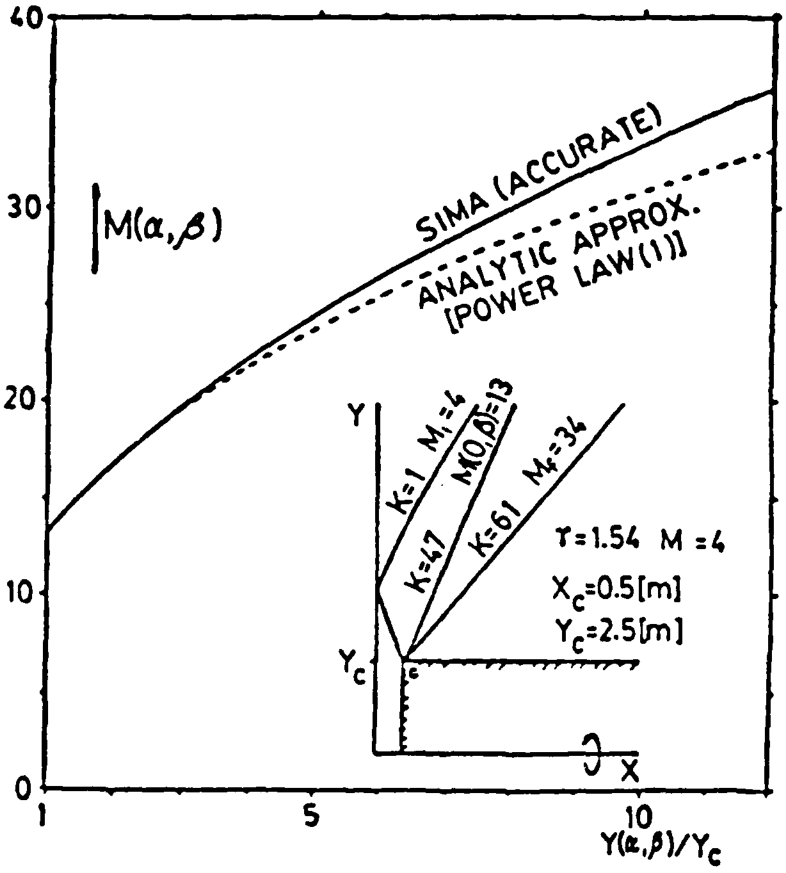


Figure 2-2. Variation of Mach Number along Characteristic Line $\beta = 13$.

## 3. AMBIENT SCATTERING

When a rocket or laser exhaust is released into space from an earth-orbiting spacecraft, it encounters an oncoming stream of ambient molecules flowing at the orbital speed of $U_A \approx 8$ (km/sec). At altitudes higher than 200 (km), the air air mean free path exceeds 250 (m), so that it is considerably larger than almost any spacecraft. Consequently, ambient molecules would hardly be subjected to a shock transition prior to their impact at the spacecraft or exhaust plume. In this chapter we describe the formulation of the first-collision model in Section 3.1 and then proceed to present the derivation of the flux integration scheme for hard-sphere collisions in Section 3.2.

### 3.1 First Collision Model

The highest ambient number density that we consider for earth-orbiting spacecrafts is $N_A = 1 \times 10^{16}$ ($m^{-3}$), which roughly corresponds to Sunspot Maximum at 200 (km) [4] . The typical laser exhaust (Table 4-1) would reach a number density of about $2 \times 10^{19}$ ($m^{-3}$) at the very high Mach number of 30. Hence, ambient flux constitutes just a slight perturbation to the near-field portion of a typical laser exhaust plume. Obviously, ambient molecules that penetrate the plume, would subsequently be entrained by the main flow. But how far do they penetrate? And would exhaust molecules scattered by them reach the spacecraft? In seeking answers to these questions, we are led to some interesting observations concerning ambient scattering.

Consider the HF laser depicted in Fig. 1-1. The spacecraft diameter is 5 (m) and the centrally located ring-symmetric nozzle is 1 (m) wide. Typical operating conditions (Table 4-1) are assumed. They are based on some experimental HF/DF laser studies conducted at TRW [5,6] . Suppose that the spacecraft axis is normal to the orbital velocity vector (normal incidence). Let the plane of incidence be the plane defined by the intersection of the spacecraft axis with the orbital velocity vector. The probability that an ambient molecule traveling in the plane of incidence would reach the spacecraft collisionlessly is $\exp(-\eta)$, where $\eta$ is its expected number of collisions with exhaust molecules. We define the number $\eta$ as "molecular thickness", in analogy to "optical thickness". So in order to determine the extent to which ambient molecules at normal incidence reach the spacecraft, we seek the distribution of radial molecular thickness as function of distance from the spacecraft mid-plane (normal to axis at its midpoint).

For this purpose we computed the ring-symmetric exhaust flow field, using a semi-inverse marching characteristics scheme [7] . The marching was in the radial direction, starting with uniform flow at the nozzle exit; the computation was carried on until it became evident that even at a distance of 20 (m) from the mid-plane, the radial molecular thickness was well over 40. The entire spacecraft was thus shielded from any ambient scattering at (or near) normal incidence. This shielding effect has two significant implications which we discuss briefly below.

(a) It is present only during stationary exhaust flow. At startup and shutdown phases, ambient scattering may be substantial even at normal incidence.

(b) During the stationary phase, ambient scattering is substantial only at attitude angles that enable ambient molecules to reach the vicinity of the plume by traveling through "molecularly thin" cavitation regions that flank the plume. We thus anticipate a decisive dependence of ambient scattering on attitude variations, whenever those variations steer the spacecraft into or out of a shielded posture.

As a first attempt at a quantitative estimate of ambient scattering flux, we have formulated a simple first-collision model of this effect. In the sequel we present an outline of the model, along with some sample results evaluated for an HF laser configuration identical to that considered for the shielding effect mentioned above.

The basic idea is the following. Ambient molecules entering an exhaust plume, require several collisions to become fully "accommodated" with the main flow (i.e., to be entrained by the main flow at the prevailing flow velocity and temperature). One may reasonably approximate this process by considering just one collision - the first.

With the help of some additional assumptions, we were able to derive a closed form expression for the flux of exhaust molecules that arrive at the spacecraft following a first collision with an ambient molecule. The main assumptions of this model are :

(1) FIRST COLLISIONS: Only first collisions for either ambient or exhaust molecules are considered. Hard-spheres elastic collisions are assumed. Upon a second collision of either an ambient or an exhaust molecule, it is considered "lost" (i.e., it joins the main flow). Collisions of ambient molecules with spacecraft surfaces are ignored. Ambient molecules are assumed to traverse cavitation regions collisionlessly.

(2) COLD FLOW: The oncoming ambient air flow is deemed "cold"; i.e., all molecules move at the uniform orbital velocity. The same "cold" assumption is applied to the exhaust flow, since most ambient scattering takes place at plume regions of very high Mach numbers (well over 10, in the present case).

(3) CRW Flow Field: ring-symmetric CRW flow field is determined from the power-law approximation described in Ch. 2 above. This approximation approaches Prandtl-Meyer flow at points whose distance from the nozzle lip is much smaller than the spacecraft radius.

Based on these assumptions, ambient scattering is represented as a source term for side-scattered exhaust molecules, distributed throughout the lip-centered rarefaction fan. The total flux arriving at a specified point on the cylindrical spacecraft is readily computed by integrating numerically that source distribution over the entire ring-fan.

The highlights of the spatial integration scheme (Fig. 3-1) are as follows. The limiting characteristic surface ($M = \infty$) of the ring-symmetric CRW is divided into surface elements formed by dividing the surface into a set of ring-strips which are subdivided in the circumferential (azimuthal) direction ($\varphi$) into surface elements. The line-of-sight ($\vec{\Omega}$) from the "target point" on the spacecraft to the center of each surface element is extended into the ring-symmetric CRW, and flux integration using the first-collision source term with appropriate weight factors is performed along this line until convergence is attained. Contributions from each surface element are summed, taking care to disregard portions of the ring-symmetric CRW that are shadowed by the cylindrical spacecraft (either the line-of-sight or the trajectory of oncoming ambient molecules may be shadowed). Some further details of the flux integration scheme and hard-spheres collisions are provided in Section 3.2 below.

### 3.2 Flux Integration Scheme

The description of the first collision model is hereby supplemented with an outline of the expressions used in the flux integration and their derivation. The integration scheme for flux arriving at point $\mathbf{X}_s$ on the spacecraft is depicted in Fig. 3-1. Note that only the plane of incidence is shown in Fig. 3-1; at other azimuth angles the geometry is not co-planar, so 3-D geometrical expressions are used to get the coordinates ($\psi$,$\varphi$ and radial distancete $(y^2 + z^2)^{1/2}$) from $\vec{\Omega}$ and $\mathbf{S}$; the derivation of these geometrical relations is straightforward, so that we omit these details in the present report. The total number flux $\mathbf{Q}_i(\mathbf{X}_s)$ of i exhaust molecules arriving at point $\mathbf{X}_s$ is given by the following expression :

$$Q_i(X_s) = \int d^3\vec{\Omega}\, \cos\alpha_s \sum_k \int_0^{\infty} dS\, \sigma_{ik}\, h_i\, N(S)\, h_k\, N_A \left|\vec{U}(S) - \vec{U}_A\right| \exp[-\eta_k(S)]\, P_{ik}(S, -\vec{\Omega}) \exp[-\eta_{ik}(S)]$$

$$\eta_k(S) = \sum_i \int_0^{t(S)} dt'\, \sigma_{ik}\, h_i\, N(t') \left|\vec{U}(t') - \vec{U}_A\right| / \left|\vec{U}_A\right| \tag{3-1}$$

$$\eta_{ik}(S) = \sum_j \int_0^{S} dS'\, \sigma_{ij}\, h_j\, N(S') \left|\vec{U}_{ik}(S) - \vec{U}(S')\right| / \left|\vec{U}_{ik}(S)\right|$$

$(\,)_i$ $(\,)_j$ – Exhaust species $(\,)_k$ – Ambient species

These expressions are interpreted as follows. The collision depicted in Fig. 3-1 is between exhaust molecule $m_i$ and ambient molecule $m_k$. The exhaust molar fractions $h_i$ and ambient molar fractions $h_k$ are assumed uniformly constant, and so are the ambient velocity $\vec{U}_A$ and number density $N_A$. The exhaust velocity $\vec{U}(S)$ and number density $N(S)$ are function of the location in the flow field defined by $\vec{\Omega}$ and S. These flow variables are computed by first evaluating the coordinates of point $\vec{\Omega}$.S (Fig. 3-1) in the ring-symmetric CRW from the 3-D geometry, and then employing the power-law approximation outlined in Ch. 2 above, to get all flow variables for a ring-symmetric CRW. In this computation we exploit the fact that characteristic lines fanning out from the nozzle lip are nearly straight lines at the low pressure side of the ring-symmetric CRW.

The $\vec{\Omega}$ integration is performed numerically according to the scheme outlined in Section 3.1 above, as a summation over elements of solid angle ($\Delta^3\vec{\Omega}$) subtended by area elements on the limiting characteristic cone ($\psi = \psi_f$).

The S integration is considerably more complex. The integrand for this integration is derived as follows. Denote by L the line-of-sight distance between point $X_s$ and fan point $\vec{\Omega}$.S. A volume element at the fan point is given by $\Delta v = L^2\, \Delta S\, \Delta^3\vec{\Omega}$. The number of ik pair collisions in $\Delta v$ per unit time is $\sigma_{ik}\, h_i\, N(S)\, h_k\, N_A \left|\vec{U}(S) - \vec{U}_A\right| \exp[-\eta_k(S)]\, \Delta v$, where $\eta_k(S)$ denotes the expected number of collisions of ambient molecule k with any exhaust molecule, between its point of entry into the plume and point $\vec{\Omega}$.S. We now multiply this term by $\exp[-\eta_{ik}(S)]$ which is the probability that exhaust molecule i scattered by ambient molecule k would travel from point $\vec{\Omega}$.S to point $X_s$ collisionlessly, where $\eta_{ik}(S)$ is the expected number of collisions for this path segment. (Note that in Eq. (3-1) the summation in the expression for $\eta_{ik}(S)$ is over all exhaust species j).

The final step in constructing the integrand for the S integration involves the post-collision directional distribution function $P_{ik}(S,-\vec{\Omega})$, whose derivation will be given in the sequel. We multiply the integrand by $P_{ik}(S,-\vec{\Omega})\,\Delta^3\vec{\Omega}_c$ which is the fraction of i exhaust molecules scattered by k ambient molecules into a solid angle element $\Delta^3\vec{\Omega}_c$ about the unit vector $-\vec{\Omega}$. Considering the flux arriving at a surface area element $\Delta A_s$ around point $X_s$, the solid angle element subtended by $\Delta A_s$ is $\Delta^3\vec{\Omega}_c = \Delta A_s \cos\alpha_s / L^2$. Eq. (3-1) for $Q_i(X_s)$ now follows upon dividing the resulting expression by $\Delta A_s$, thus referring the arriving flux to a unit area at the point of arrival $X_s$.

Numerically, the S integration was performed using the classical Runge-Kutta scheme (fourth order). The integration for $\eta_{ik}(S)$ and $\eta_k(S)$ has to be repeated at each point S. We found reasonable convergence with 4 points in the $\eta_k(S)$ integration and 6 points in the azimuth integration. The S integration was terminated when convergence was attained (this is the meaning of the upper limit $\infty$ in the S integral in Eq. (3-1)). The summation over new strips on the limiting cone ($\psi = \psi_f$) was also terminated upon convergence. The CPU time consumed per target point was about 100 (sec) on IBM 3033 mainframe.

We now take up the derivation of an expression for the post-collision directional distribution function $P_{ik}(S,-\vec{\Omega})$, which we denote hereafter as $P(-\vec{\Omega})$. We adopt the pair-collision notation presented in Fig. 3-2 for the hard-sphere collision analysis.

As a consequence of conservation of momentum and energy (elastic collisions), the center-of-mass velocity $\vec{C}_m$ and the magnitude of the relative velocity $\vec{C}_r$ are unchanged by the collision [8] . The post-collision velocities are given by :

$$\begin{aligned}
&\vec{C}_1^* = \vec{C}_m + \mu_2\vec{C}_r^* && \vec{C}_2^* = \vec{C}_m - \mu_1\vec{C}_r^* \\
&\vec{C}_r = \vec{C}_1 - \vec{C}_2 && \vec{C}_r^* = \vec{C}_1^* - \vec{C}_2^* \\
&\mu_1 = m_1/(m_1+m_2) && \mu_2 = m_2/(m_1+m_2) \\
&\vec{C}_m = \mu_1\vec{C}_1 + \mu_2\vec{C}_2 && |\vec{C}_r^*| = |\vec{C}_r|
\end{aligned} \tag{3-2}$$

The only free parameter in the expressions for post-collision velocities is the orientation of the post-collision relative velocity $\vec{C}_r$. This orientation is uniformly likely to be in any direction in space when hard-spheres collision is assumed [8] , as represented by the spherical scattering envelope in

Fig. 3-3. The probability of obtaining $\vec{C}_1^*$ in solid angle element $\Delta^3\vec{\Omega}$ about $-\vec{\Omega}$ (Fig. 3-3) is given by :

$$P(-\vec{\Omega}) = \left(1/4\pi|\mu_2\vec{C}_r|^2\right)\left(\Delta A/\Delta^3\vec{\Omega}\right) = \left(1/4\pi|\cos\delta|\right)\left(|\vec{C}_1^*|^2/|\mu_2\vec{C}_r|^2\right) \tag{3-3}$$

where $\Delta A$ is an area element on the scattering envelope, whose projection on a plane normal to $\vec{\Omega}$ is $\Delta A\ |\cos\delta|$. We note that the origin of $\vec{C}_m$ in Fig. 3-3 is external to the scattering envelope, resulting in two possible scattering elements on the sphere. In all the cases that we computed, however (see Ch. 4 below), that point was found to be always internal, so that there was only a single scattering solution with post-collision velocity $\vec{U}_{ik}(S)$ pointing at the spacecraft for any ik pair collision.

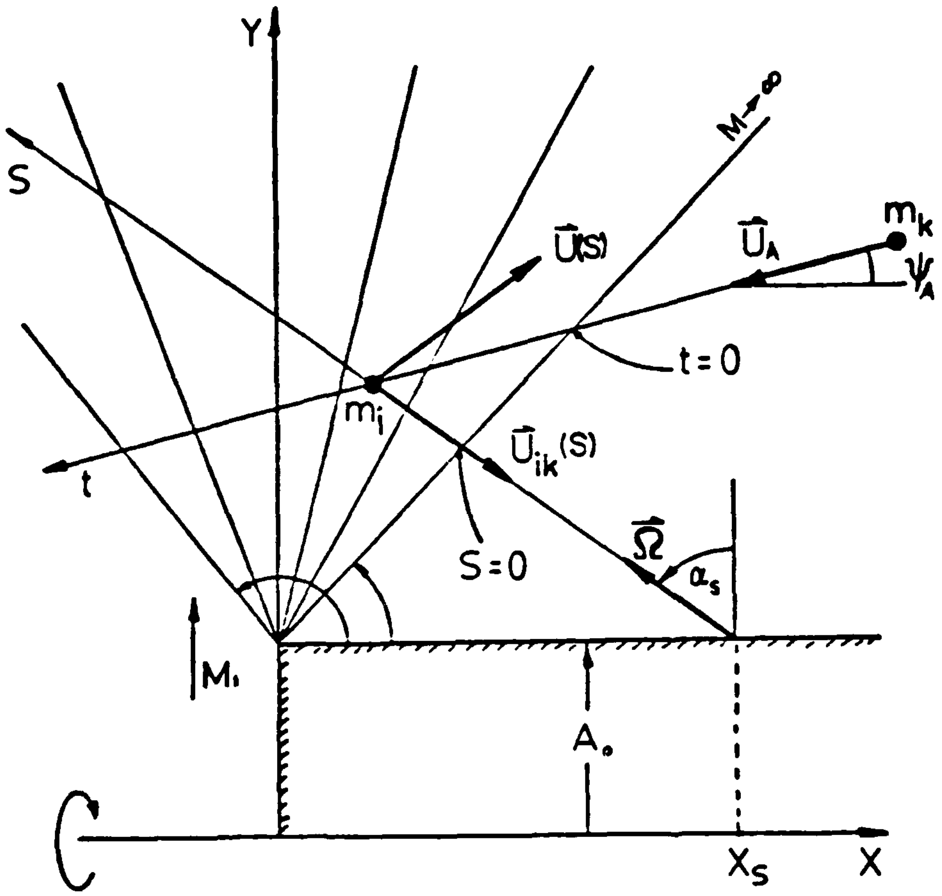


Figure 3-1. Incidence-Plane Description of Flux Integration Scheme.

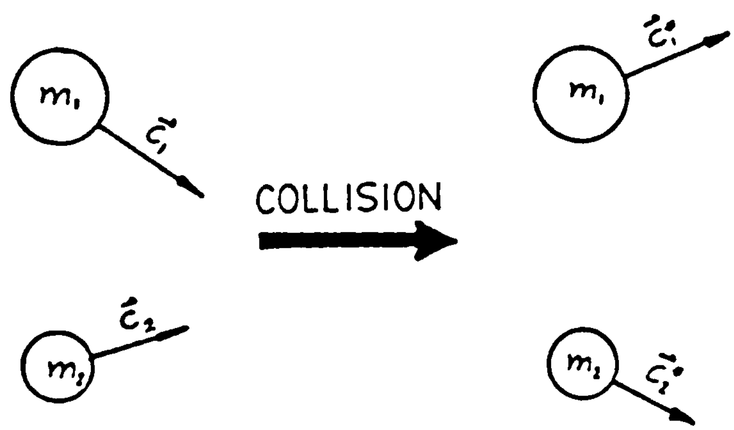


Figure 3-2. Hard-Spheres Collision Notation.

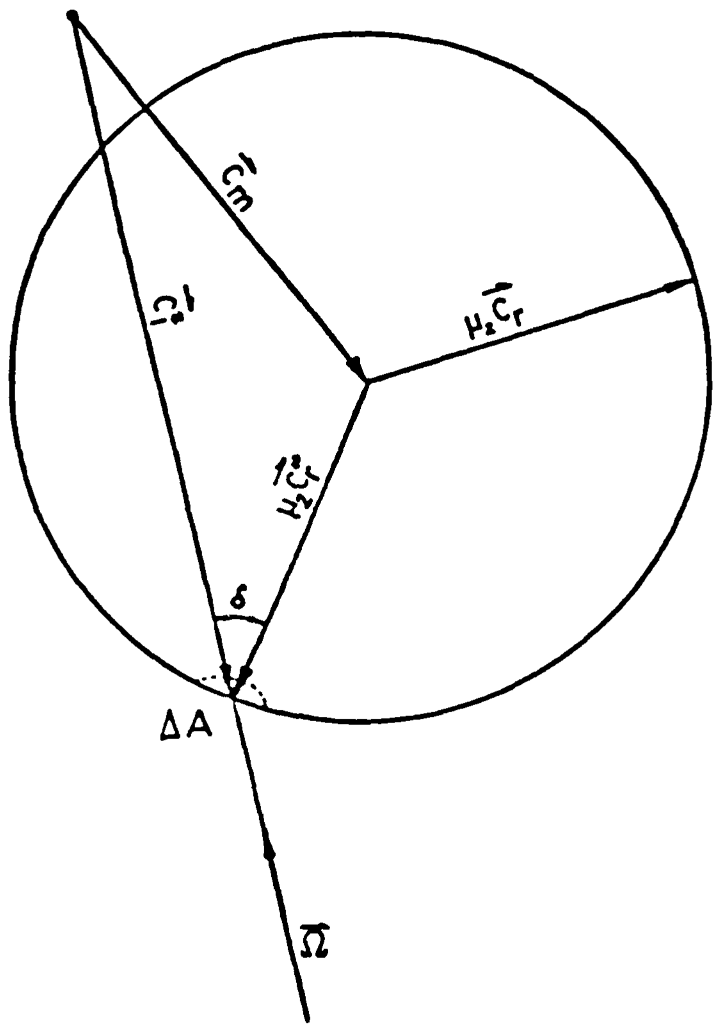


Figure 3-3. Scattering Envelope for Hard-Spheres Collision.

## 4. RESULTS AND DISCUSSION

We performed several computations of return flux generated by ambient scattering, aimed at demonstrating the expected flux level and its variation with spacecraft target point and orbital attitude angles. In all these computations we assumed that the exhaust flow is as in the typical HF/DF laser case (Table 4-1 below), and that the ambient density and velocity are $N_A = 1 \times 10^{16}$ (molecules/m$^3$) and $U_A = 8$ (km/sec). As an approximation we further assumed that the sole ambient species is molecular nitrogen (molecular weight $W_A = 28$) and that all binary collision cross-sections are uniformly given by $\sigma = \pi D^2$, where **D** is the molecular diameter (Table 4-1). In each computation we evaluated the combined HF+DF flux by assuming that the molar fraction of DF is zero and the molar fraction of HF is the combined value for both species (Table 4-1) : .091 + .135 = .226 . This is justified by the relatively small difference in molecular weight (just 5%) between these two species.

Three sets of flux computation were performed as follows :

(a) Incidence-plane ($\varphi_A = 0$) target points at various distances from the nozzle lip ($X_s = .1$ to $X_s = 10$ (m)), and at constant incidence angle ($\psi_A = 20°$). The results are shown in Fig. 4-1. We observe that the flux is fairly insensitive to $X_s$. Also shown in Fig. 4-1 are flux computations where the ring-symmetric CRW flow is approximated as a planar CRW (Prandtl-Meyer flow), rather than the power-law as in Eq. (2-1) above. The planar case exhibits a somewhat higher flux, particularly at large $X_s$.

(b) Incidence-plane ($\varphi_A = 0$) target points at $X_s = 1$ (m) and at various incidence angles ($\psi_A = 0$ to $\psi_A = 40°$). A polar representation of the results is given in Fig. 4-2. Note the sharp decrease in flux as the incidence angle $\psi_A$ approaches the plume limiting angle $\psi_f = 41°$.

(c) Azimuth angle variation ($\varphi_A = 0$ to $\varphi_A = 180°$) at a constant location ($X_s = 1$ (m)) and at a constant angle of incidence ($\psi_A = 20°$). A polar representation of the results is given in Fig. 4-3. Observe that flux becomes sensitive to azimuth angle $\varphi_A$ only past $\varphi_A = 90°$, where shadowing by the cylindrical spacecraft becomes increasingly dominant.

In addition to return flux we also computed the rms velocity of the arriving molecules. For the target points in group (a), the rms velocity varied between 6000 and 6600 (m/sec) (the higher velocity at smaller $X_s$), which corresponds to a kinetic energy of about 4 (ev) per molecule (HF).

The maximum return flux arriving at the spacecraft is about $0.15 \times 10^{19}$ (molecules/m$^2$sec), which corresponds to a surface deposition rate of about 300 monolayers (HF + DF) per hour. This level of contaminating flux may seem to be not outright negligible; however, since return flux is proportional to ambient density, it will be scaled down considerably at higher altitudes (and lower ambient densities).

We observe that the maximum return flux constitutes a fraction of about 2% of the incident ambient flux. This return flux ratio is roughly maintained at almost all target points and attitude angles in groups (a), (b) and (c). The only exceptions are incidence angles near the limiting cone ($\psi = \psi_f$) or at azimuth angles $\varphi_A > 125°$ where shadowing becomes dominant. This observation is interpreted as follows.

Consider the total solid angle subtended by the limiting cone (considered to be infinitely extended in the axial direction) as viewed from a target point (for all lines-of-sight $\vec{\Omega}$ pointing outward of the cylindrical spacecraft surface). It is independent of target location due to the "self-similar" geometry. During each flux computation, we also evaluated the total solid angle subtended by that segment of the cone over which the flux integration was actually performed (see Section 3.2). It was found out that for all but the "shadowed" cases ($\varphi_A > 125°$), this solid angle constituted a fraction of $86 \pm 1$% of the solid angle subtended by the infinite cone. We interpret this result as a hint that geometrical "view factors" arising in the course of the flux integration, are not the dominant factor in determining the 2% level of flux ratio. What then are the dominant factors?

For a possible explanation we turn to the flux integration scheme presented in Section 3.2. The flux ratio is obtained upon dividing the integrand in Eq. (3-1) by $N_A U_A$ and setting $h_k = 1$ (since we assume a single species air). The major factors in the flux ratio integrand appear to be the no-collision probabilities $\exp[-\eta_{ik}(S)]$ and $\exp[-\eta_k(S)]$, and the post-collision directional distribution function $P_{ik}(S, -\vec{\Omega})$. The flux-averaged values of these functions in the group (a) computations were found to be as follows : $P_{ik}(S, -\vec{\Omega}) = .09$ to $.10$ . $\eta_{ik}(S) = .42$ to $.54$ and $\eta_k(S) = .35$ to $.47$. The flux-averaged Mach number for group (a) points exhibited a much larger variation : between 30 and 80, with the higher Mach numbers obtained at further target points.

These results are interpreted as follows. The ambient no-collision probability $\exp[-\eta_k(S)]$ is sufficiently close to unity, so that in an order-of-magnitude analysis such as the present one, we may disregard this factor. If the velocity ratio in the $\eta_{ik}(S)$ integral of Eq. (3-1) is assumed to be unity (its average value for group (a) points is about 1.4), then the differential in the flux S integration becomes

$\sigma N(S)dS = d\eta_{ik}(S)$. This implies that the flux **S** integration results in some average value of the only remaining factor : $h_i P_{ik}(S, -\vec{\Omega})$. Since the $\vec{\Omega}$ integration introduces a factor of order unity, the order-of-magnitude estimate for the arriving-to-incident flux ratio is $[h_i P_{ik}(S, -\vec{\Omega})]_{av}$ . The value of this estimate is $[h_i P_{ik}(S, -\vec{\Omega})]_{av} = .226 \times .09 \approx .02$, which is about equal to the actual flux ratio for target points in group (a).

When an exhaust flow and orbital parameters (velocity and attitude) are specified, $P_{ik}(S, -\vec{\Omega})$ depends on the choice of molecular collision model (we chose hard spheres), while $h_i$ is uniformly constant. The foregoing reasoning thus establishes the collision model as a significant factor in determining ambient scattering flux levels, to the extent that $P_{ik}(S, -\vec{\Omega})$ is sensitive to the choice of model.

Table 4-1. Typical Operating Conditions of HF/DF Laser Exhaust

| | | | | | |
|---|---|---|---|---|---|
| Mole fractions | [H ] = .091 | [HF] = .091 | $[H_2]$ = .104 | [DF] = .135 | [He] = .579 |
| Average molecular weight | 7.14 | | | | |
| Specific heats ratio | 1.54 | | | | |
| Stagnation temperature and density | 1400 (K)<br>.0075 (kg/m$^3$) | | | | |
| Exit Mach number | 4.0 | | | | |
| Molecular diameter (hard spheres) | $2.5 \times 10^{-10}$ (m) | | | | |
| Spacecraft diameter | 5.0 (m) | | | | |
| Nozzle aperture | 1.0 (m) | | | | |

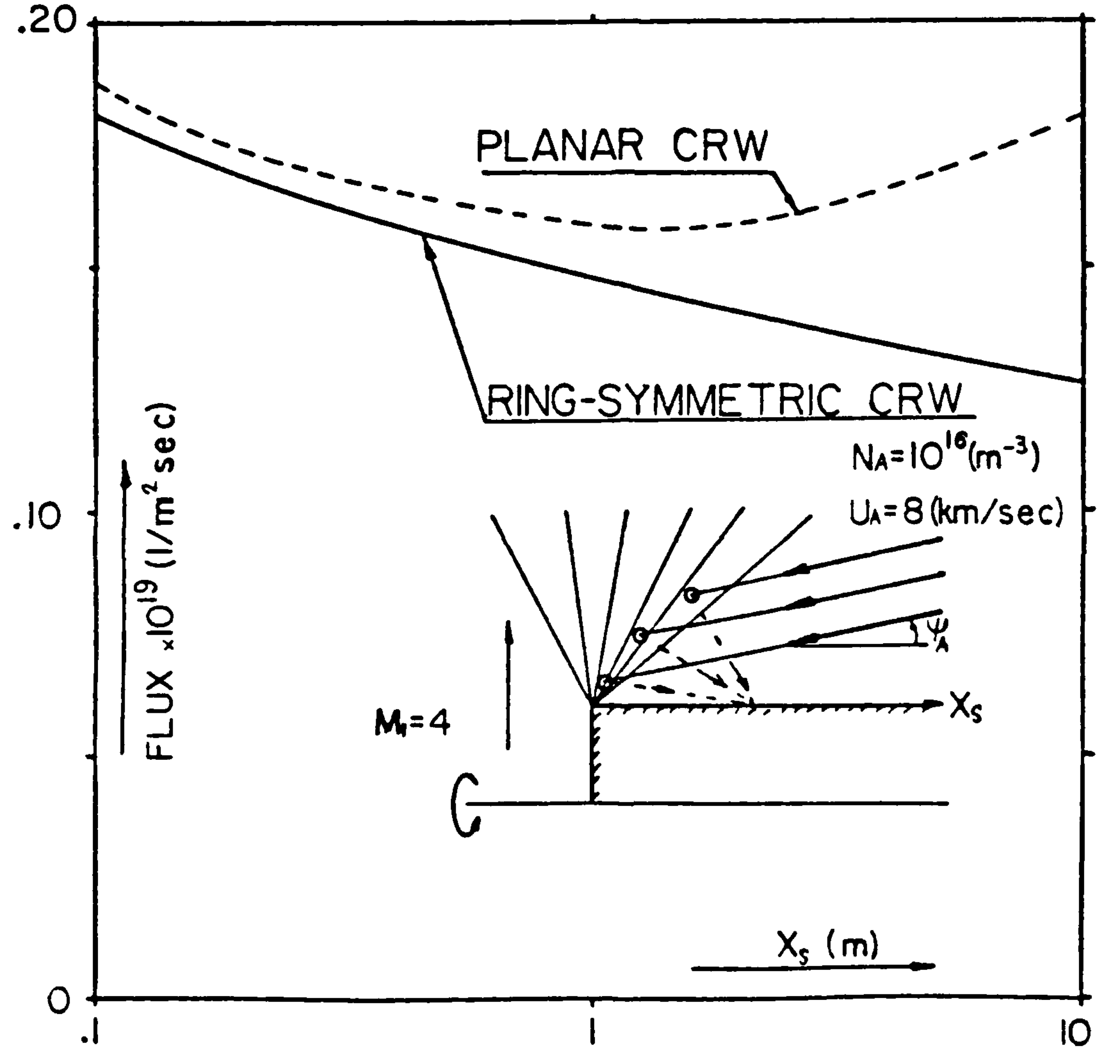


Figure 4-1. Variation of Return Flux with Target Point ($X_s$). Target Point at Incidence-Plane ($\varphi_A = 0$) and Constant Incidence-Angle ($\psi_A = 20°$).

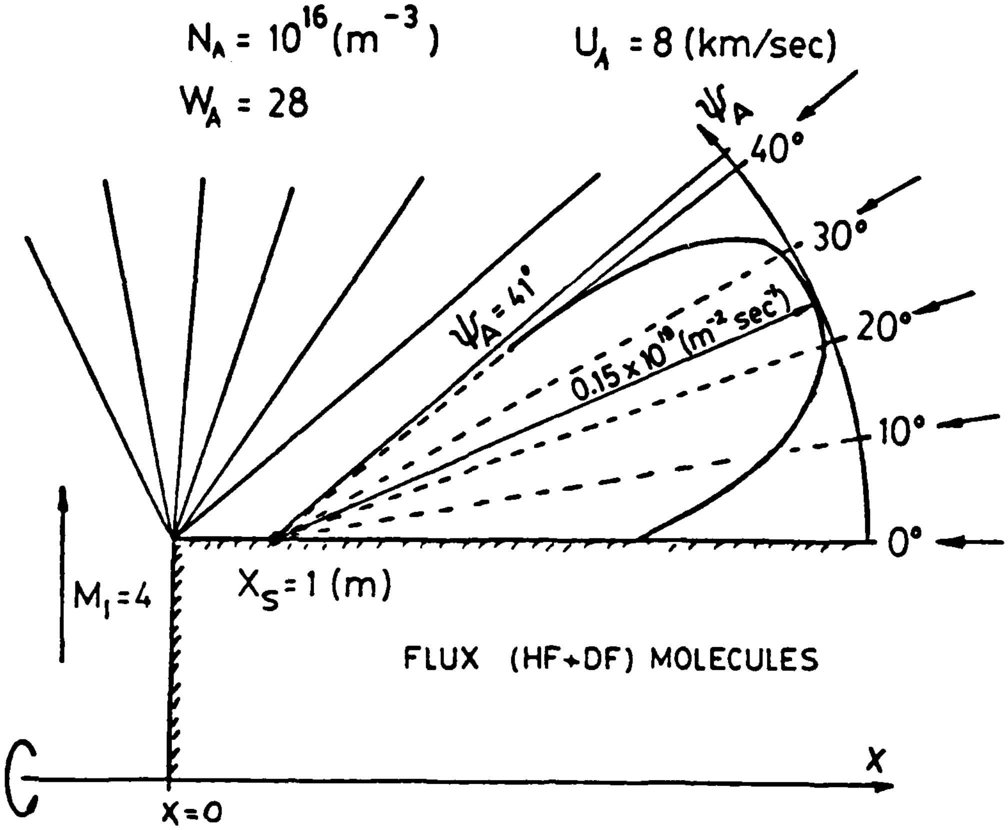


Figure 4-2. Variation of Return Flux with Ambient Incidence Angle ($\psi_A$). Fixed Target Point ($X_s = 1$ m) Located at Incidence-Plane ($\varphi_A = 0$).

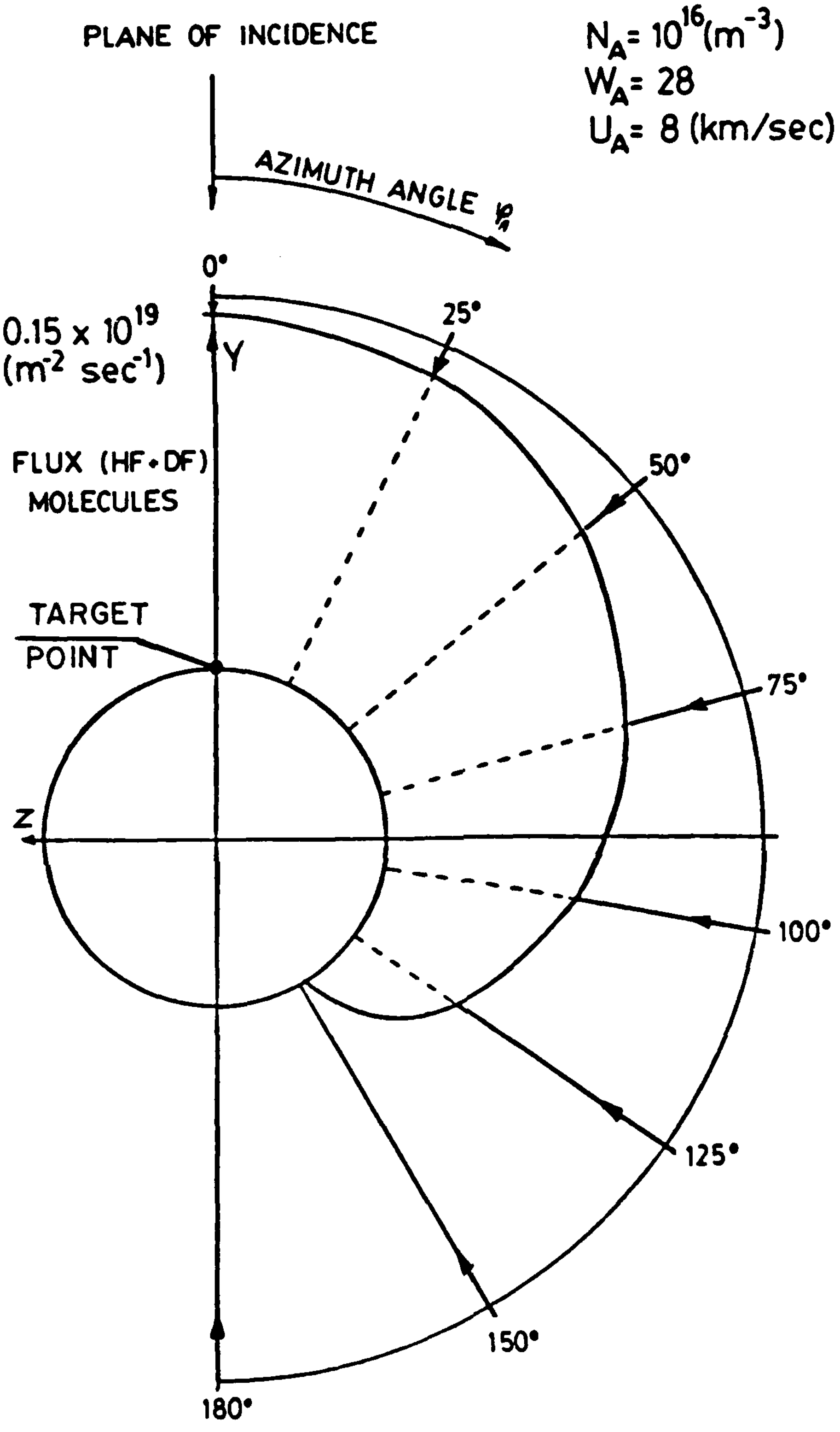


Figure 4-3. Variation of Return Flux with Ambient Azimuth Angle ($\varphi_A$). Fixed Target Point ($X_s = 1$ m) and Ambient Incidence Angle ($\psi_A = 20°$).

## 5. SPACECRAFT CHARGING

Spacecraft charging is a major concern to spacecraft designers, particularly for missions in GEO and to a lesser extent also in LEO. The exhaust plume of an HF/DF laser operating in the ionosphere (300 to 1000 km altitude) may modify significantly the pre-firing charging pattern of the spacecraft. Two classes of effects may lead to charging modification; they are:

(a) The exhaust contains large concentrations of HF and DF molecules which are highly electronegative. They may be readily ionized by environmental electrons and change the existing spacecraft charging pattern.

(b) When the spacecraft is oriented obliquely relative to its orbital velocity and the ambient plasma impinges at the plume boundary, the plume will cast a "shadow" on the downstream side, leading to a very dissimilar charging fluxes on the upstream and downstream halves of the spacecraft.

The knowledge gained in analyzing the ambient scattering effect can be applied to the assessment of the effects of ionospheric plasma on spacecraft charging. We first consider the upstream side of the spacecraft as mentioned in (a) above.

We contend that the exhaust-plasma interaction will not drastically alter the charging pattern of the upstream half. This assessment is established as follows. Consider the fact that ionospheric plasma has a particle number density no higher than $10^{12}$ ($m^{-3}$) and energy per particle of at most 1 (ev) (excluding the auroral plasma of polar zones or events of sun storms, where the energy per particle is much higher). Significantly, the Debye length at the highest plasma density is very small: only about $10^{-3}$ (m); the largest Debye length in the ionosphere is $10^{-1}$ (m) [9]. Ion thermal velocity is typically lower than orbital velocity, but electron velocity is considerably higher than orbital velocity (at 1 ev the electron velocity is about $U_e = 6 \times 10^5$ m/sec). Hence, ions would typically impinge at the plume as a uniform ion beam with the orbital velocity (like ambient molecules), while electrons are expected to impinge at the plume with their random-oriented thermal velocity.

In view of the results of ambient scattering analysis (Ch. 3 and 4 above), and since ions are subject to similar collision process with exhaust molecules as neutrals, ions will be stopped at the plume fringes much like ambient molecules. By virtue of the small Debye length (typically much smaller than the stopping distance), electrons would not penetrate any further than ions, regardless of their collision cross-section with exhaust molecules. The familiar plasma sheath that forms at a solid surface, is hence replaced at the plume/plasma boundary by a typically neutral layer whose thickness is of the order of an ion/neutral mean free path, but much larger than the Debye length. Only at the upper altitude range of the ionosphere does the Debye length become comparable to a plume boundary mean free path (about .1 m), but there plasma density and flux are several orders of magnitude lower and charging modification is not likely to be significant at the relatively short firing duration of about 5 minutes.

Elastically scattered ions can be deflected towards the spacecraft as a result of elastic collisions with exhaust molecules, much like neutrals. Referring to our analysis of the return-to-ambient flux ratio (Ch. 4 above), it is clear that the relevant ratio here will be about $1/4\pi$, i.e., of the order of 10% (this is due primarily to the role played by the elastic directional distribution function – see Ch. 4). A change in the plasma-to-surface current of that order is hence possible, but unlikely to affect spacecraft design or operation significantly. The reason is that a design capable of smoothing away the inhomogeneous charge flux at oblique attitudes, will not be sensitive to a change in flux pattern of the order of 10% (in other words, potential differences may be amplified by 10%, which is hardly likely in a sound design to bring about arcing or other threshold phenomena).

Another effect which may potentially be significant in the upstream half is generation of electronegative species ($HF^-$, $DF^-$) by plasma electrons impinging at the plume. *In the sequel, we* examine the magnitude of this effect, concluding that it is negligible.

This estimate is best done by considering $\dot{N}^-$, which is the rate of production of $HF^-$ and $DF^-$ per unit volume, at a typical point in the exhaust where local Mach number is $M = 30$ (this is typically the lowest average Mach number for the plume region where ambient scattering takes place – see Ch. 4 above). Since energy is released by the electronegative ion formation, the reaction involves a third body as follows :

$$HF + e^- + M \rightarrow HF^- + M \qquad (5\text{-}1)$$

where $M$ is the third body molecule. We assume a simplified classical kinetic model for this reaction, as follows. The pair HF/M collide with a frequency proportional to the local number density and HF molar fraction, and to the average relative velocity. An electronegative ion formation can occur only if an electron collides with the pair during their collision, which lasts $t_c = D/\bar{C}_r$, where $\bar{C}_r$ is the average relative pair velocity. Based on this classical model, and assuming the same cross-section for electronegative ion formation as for elastic HF/M collisions, the volume rate of electronegative ion generation is given by :

$$\dot{N}^{-} = (\pi D^3 N)\, Nh\, (\pi D^2 U_e N_e) \qquad (5\text{-}2)$$

where $(\pi D^3 N)$ is the probability that a certain HF or DF molecule will be in contact (**D** being molecular hard-sphere diameter) with any other exhaust molecule (whose number density is N). When $(\pi D^3 N)$ is multiplied by **h**N, where **h** is the HF+DF molar fraction (Table 4-1), the combined term reads as the number of colliding HF/M pairs per unit volume. Assuming the electronegative formation cross-section is also $\pi D^2$, the factor $\pi D^2 U_e N_e$ where $U_e$ and $N_e$ are electron velocity and number density, renders the expression for electronegative generation rate per unit volume. We note that $\overline{C}_r$ cancels out in deriving Eq. (5-2), so that $\dot{N}^{-}$ does not depend on temperature. This supports the use of the kinetic approximation in regions of continuum breakdown (plume fringes are such regions).

How is the relative magnitude of $\dot{N}^{-}$ decided? To do that we multiply $\dot{N}^{-}$ by $\lambda = 1/\pi D^2 N$, which is the mean free path for a fast moving particle that penetrates the plume. This expression is justified by the fact that most incident particles do collide within a distance of order λ, and when the particles are plasma ions, electrons will adhere to ion spatial distribution by virtue of the small Debye length (smaller than λ). Thus, $\lambda \dot{N}^{-}$ is the rate of electronegative ion generation per unit area of plume boundary. The ratio $\beta^{-}$ between this rate and the incident electron flux is :

$$\beta^{-} = \lambda \dot{N}^{-} / N_e U_e = (\pi D^3 N) h = 2.2 \times 10^{-10} \qquad (5\text{-}3)$$

where $N = 2 \times 10^{19}$ ($m^{-3}$) which corresponds to Mach number **M** = 30 in the typical case (Table 4-1). The fraction of electron flux captured by HF and DF exhaust molecules to form electronegative ions is so small (due to the pair-formation term $(\pi D^3 N)$), that it cannot appreciably alter the charging flux distribution at the spacecraft surface.

Another possible effect is the recoil of $HF^{-}$ or $DF^{-}$ that occurs due to energy released in the electronegative formation reaction. The recoiling species might conceivably reach the surface and contaminate it. The magnitude of the recoil flux is certainly no larger than $\beta^{-} U_e N_e = 1300$ ($m^{-2}$ $sec^{-1}$), where we assume the worst case flux : $N_e = 10^{12}$, $U_e = 6 \times 10^5$ (m/sec) which corresponds to about 1 ev energy per electron. This flux level is about $3 \times 10^{-13}$ monolayers of $HF^{-}$ and $DF^{-}$ per hour, so that its contribution to surface contamination is utterly negligible.

The second kind of charging effects (item (b) above) is due to the fact that the exhaust plume is impenetrable to ambient plasma (within a range of sufficiently small distance from the spacecraft, so that no extensive diluting of the plume has taken place). The downstream half of the spacecraft in oblique attitude will be in the "shadow" with respect to incident plasma. As a first approximation we may assume zero plasma flux at the shadowed surface. More accurately, this portion of the spacecraft will be subject to a plasma wake flow. However, it is quite difficult to determine the charging phenomena that take place in such a wake, as indicated by a recent work on solar sails in LEO [9] . Thus, a zero flux at the downstream half seems a practical design assumption.

Can adverse charging effects occur as a result of shadowing the downstream half? This question can be discussed only qualitatively. The reason is that a quantitative analysis requires a lumped-circuit model of the spacecraft external surface [10] . Since such a concrete design is not available, we can only discuss this question qualitatively. Obviously, assuming zero flux to the downstream half during the envisioned 5 minutes of laser firing duration, and requiring that no appreciable voltages between the two halves will evolve, leads to the stipulation that the equivalent-circuit Capacitance × Resistance should be much smaller than the firing duration.

## 6. CONCLUDING REMARKS

Our major quantitative conclusion is that for the relatively high ambient density assumed ($N_A = 1 \times 10^{16}$ molecules/m$^3$ which represents Sunspot Maximum at about 200 km) and for the typical HF/DF laser exhaust (Table 4-1), the HF+DF flux backscattered by ambient molecules is several hundred monolayers per hour. This flux level may seem as not outright negligible. However, since ambient scattering flux is proportional to ambient density, it will be scaled down considerably at the lower ambient densities of higher orbital altitudes.

The operational scenario for HF/DF laser envisions 4 or 5 minutes total operating time; hence the contamination by ambient scattering may not be serious due to short operating time.

The effects of laser exhaust plume on spacecraft charging in the ionosphere were examined. It was concluded that the rate of electronegative (**$HF^-$** and **$DF^-$**) production by impinging electrons was negligible; the low rate is a consequence of the assumption that a third body is required to interact simultaneously with the HF/e or DF/e pair. No significant modification of charging pattern is anticipated. However, at oblique orbital attitudes, the downstream half of the spacecraft will be shadowed from the oncoming ambient plasma. This fact has to be reckoned with in designing a ring-symmetric laser spacecraft.

The emphasis in this work was on the method rather than on results. The first-collision model was demonstrated to be simple to implement in a code. It is considerably simpler than the more general and potentially more accurate Monte Carlo methods commonly used for simulating rarefied flows (5). We found out that the molecular collision model was all important in determining the return flux level, which is hardly surprising for scattering by single collision. For the same reason, the collision model would also be dominant in a Monte Carlo simulation of the ambient scattering process.

If and when a mathematical accuracy of the first-collision approximation is established for hard-spheres, it might be possible to determine a realistic collision model by comparing computed results with measurements.

This accuracy may be established in either of two ways. One way is by comparison with accurate Monte Carlo computations (using hard-spheres collision model). The other is to seek an estimate of the error incurred by considering just first collisions and ignoring all subsequent ones. This might be achieved by accounting for second collisions in an extended first-collision model, provided a simplified scheme that will obviate the need for increase in the dimensions of the numerical flux integration can be devised. We are currently considering such second-collision approaches.

## 7. REFERENCES

[1] Bird, G. A., "Breakdown of Continuum Flow in Free Jets and Rocket Plumes", Proceedings of $12^{th}$ Symposium on Rarefied Gas Dynamics. In Volume 74, Progress in Aeronautics and Astronautics, Part II, pp.681, Sam S. Fisher, Editor. Published by AIAA, 1981.

[2] Falcovitz, J., "Analytic and Numerical Computation of Ring-Symmetric Spacecraft Exhaust Plumes", Report NPS72-86-003CR, Dec. 1986, Naval Postgraduate School, Monterey, CA 93943.

[3] Liepmann, H. W. and Roshko, A., *Elements of Gasdynamics*, John Wiley, New York, 1957.

[4] Johnson, F. S., *Satellite Environment Handbook*, Second Edition, Stanford University Press, Stanford, California, 1965.

[5] Mastrup, F., Broadwell, E., Miller, J. and Jacobs, T. A., "Hydrogen Fluoride Laser Technology Study", Technical Report AFWL-TR-72-28, October 1972.

[6] Falcovitz, J., "Transient Reactive Exhaust Flow from a Ring-Symmetric HF/DF Space Laser", Report NPS72-87-002CR, Mar. 1987, Naval Postgraduate School, Monterey, CA 93943.

[7] Falcovitz, J., "Numerical Computation of Ring-Symmetric Spacecraft Exhaust Plumes", Report NPS72-87-001CR, Jan. 1987, Naval Postgraduate School, Monterey, CA 93943.

[8] Bird, G. A., *Molecular Gas Dynamics*, Clarendon Press, Oxford, 1976.

[9] Hill, J. R., and Whipple, E. C., "Charging of Large Structures in Space with Application to the Solar Sail Spacecraft (survey)", *Journal of Spacecrafts and Rockets*, Vol. 22, pp. 245-253, 1985.

[10] Garrett, H. B., "Spacecraft Charging : A Review", pp. 167-226, in *Space Systems and Their Interactions with Earth's Environment*, Henry B. Garrett and Charles P. Pike, editors, Vol. 71 "Progress in Astronautics and Aeronautics", Published by AIAA, 1980.

# APPENDIX A. DESCRIPTION OF AMB CODE

## A.1 Description of Subroutines

We provide a list of the subroutines in the ambient flux integration code AMB for ring-symmetric cylidrical spacecrafts. Each subroutine is briefly described. Statements are identified by the FORTRAN statement number (columns 1 through 5).

MAIN PROGRAM The 300 loop is intended to enable several (NCASE) reruns with various data in each, all in a single run. Upon calling INIDAT1, parameters depending on data defined in INIDAT are re-computed. The 200 loop is over various XSV(NX) target points. In the 20 loop the flux integration begins : FLUXC is for particle flux and FLXU2C is for the rms of velocity of return flux molecules. All the MAX suffixed parameters denote values at which the integrand had the largest value.

The actual flux integration commences at statement 1 for the summation over strips of constant RF. This summation is terminated when convergence is attained (to within EPSR). The inner loop 2 is over azimuth angle PHI. Note that the target points are generally not in the plane of incidence (PHIA.NE.0), so that no symmetry can be assumed in the PHI integration, and it is performed twice in order to cover the entire range in PHI (IPAR=1 for PHI.GT.0, IPAR=2 for PHI.LT.0). The flux integration along the line-of-sight is done by calling FLUX.

INIDAT Initialization of data. There is no input file for this code. INIDAT1 is for parameters computed from the data defined by calling INIDAT.

SOF Stopping routine, called when an error is detected. Here we also trigger a system error by computing DSQRT(-1), in order to obtain a calling sequence printout by the operating system.

FLUX This routine calls SUMT for flux integration of one exhaust species at a time.

LIMIT Here we compute the point of intersection of the line-of-sight with the leading characteristic cone. If they do not intersect, the distance of the intersecting point TLIM is set to a very large number.

SUMT This is the line-of-sight integration routine. Runge-Kutta scheme is used (even though an explicit integral is computed). Note that ETAK and ETAIK have to be computed through a separate integration at each point of the line-of-sight integration. The integration step DT (T=S/RF) is re-adjusted at each integration step. The integration is terminated when convergence is attained (to within EPST).

FETA Here the integrand for the line-of-sight flux integration is evaluated. The hard-spheres collision model is used to determine the post-collision directional distribution factor PIK. The flux-average of any variable (such as UIK**2 in present version), can be computed by summing it multiplied by flux and subsequently dividing by the total arriving flux (see loop 31 in MAIN PROGRAM).

PATHIK Here the molecular thickness ETAIK of the I exhaust species scattered by the K ambient molecule, is computed by integration along the line-of-sight.

FT This routine computes the integrand for the ETAIK integration in PATHIK.

PATHK The analog to PATHIK for K ambient molecule. TAU is the normalized integration variable along the trajectory of the penetrating ambient molecule. Note that SHADOW=.TRUE. when the trajectory passes through the cylindrical spacecraft surface before entering the fan.

FTAU Computes the integrand for the ETAK integration in PATHK.

FAN Computes the fan coordinates PSI, XP, YP for a point on the line-of-sight. It is used to determine the Mach number and flow angle from the power-law approximation (see MATCH).

FANT Computes the fan coordinates PSI, XP, YP for a point on the ambient molecule trajectory.

HMSET Prepares the vector HMV(I) which is the value of the H(M) integral at a set of Mach number values (equally spaced in inverse Mach number). This vector is used to compute H(M) for an arbitrary M (see HINTER), since this function is needed in the power-law approximation of flow in a ring-symmetric fan. Subsequent routines MFUNC, HINTER, MATCH and AREAF are all used to implement this approximation.

MFUNC Computes the integrand for the H(M) integration in HMSET.

HINTER Computes H(M) for a given M, from HMV(I) by linear interpolation. Note that the interpolation is done with inverse Mach number as the independent variable.

MATCH Here the approximation to the "inverse problem" of finding the Mach number at a single point in the ring-fan is implemented. An iteration scheme is used to determine the fan characteristic passing through the given point [2] .

AREAF Mach number is computed from value of area ratio function. Newton-Raphson iterations are used.

## A.2 Listing of AMB code

```
C$OPTIONS LIST
C  AMBIENT.  SCATTERING FROM A RING PLUME BY AMBIENT AIR.
      IMPLICIT REAL*8(A-H,O-Z)
      COMMON /GAMA/G,G1,G2,G3,G4,G5,G6,G7,G8,G9,G10,G11,G12,G13,G14,G15,
     1             G16,G17,G18,G19,G20
      COMMON /PAR/C0,EN0,EM1,D,SIGMA,TLIM,DR0,EL0,Q0,T0,FACT,ALOGF,
     1            DPSI0,DTMAX,DETA0,ETALIM,XSI,XSF
      COMMON /NPAR/NPHI,IPAR,NP,NR,NX,NXS,NS,NSPEC,NS1,NS2,NTAU0,NETA0,
     1             NAMB,NCASE,ICASE,IFAN
      COMMON /GEOM/APF,PAI,PAI2,W,SW,CW,BETA,SBETA,CBETA,PSI1,SPSI1,
     1             CPSI1,PSIF,SPSIF,CPSIF,TPSIF,AK,SK,CK,A0,RF,XF,YF,ZF,
     2             PHISOF,PHIF,SPHIF,CPHIF,DYMIN,RMIN,XS,DIST,X0,Y0,Z0,
     3             DY0,DEG,PSIN,ST1,CT1,OMEGX,OMEGY,OMEGZ,XSV(21)
      COMMON /EPSIL/EPSETA,EPST,EPSR
      COMMON /EXTREM/TEXT(5),ETAEXT(5),ETAKXT(5),PHIEXT(5),
     1               PSIEXT(5),EMEXT(5),FEXT(5),WEXT(5),
     2               TMAX(5),ETAKMX(5),ETAMAX(5),PSIMAX(5),
     3               EMMAX(5),FMAX(5),
     4               RFMAX(5),PHIFMX(5),PHIMAX(5),WMAX(5)
      COMMON /COUNTS/ICONTC,ICONTT,ICNTOT,ICNTMX,IQTOT(5),ISHAD(5)
      COMMON /SPEC/WAV,XC(5),WC(5),WRC(5),XNAME(5),QFC(5),QDC(5),
     1             QU2C(5),FLUXC(5),OMEGA(5),FLXU2C(5),URMSC(5)
      COMMON /AMBIEN/ENA,UA,PSIA,PHIA,HA(3),WA(3),
     1               UAX,UAY,UAZ,AA,BA,CA,RA,XA,YA,ZA,SHADOW
      COMMON /POINT/XP,YP,XCOR,YCOR
      LOGICAL SHADOW
      DIMENSION DSUMF(5),DSUMD(5),DSUMAX(5),DSUMU2(5)
      NCASE=1
      DO 300 ICASE=1,NCASE
      CALL INIDAT
      GO TO (301,302,303,304,305,306,307,308,309,310,
     1       311,312,313,314,315,316,317,318,319,320),ICASE
  301 CONTINUE
      IFAN=1
      NXS=3
      XSI=0.1D0
      GO TO 399
  302 CONTINUE
      PHIA=20.D0/DEG
      GO TO 399
  303 CONTINUE
      PHIA=50.D0/DEG
      GO TO 399
  304 CONTINUE
      PHIA=75.D0/DEG
      GO TO 399
  305 CONTINUE
      PHIA=100.D0/DEG
      GO TO 399
  306 CONTINUE
      PHIA=125.D0/DEG
      GO TO 399
  307 CONTINUE
      PHIA=150.D0/DEG
      GO TO 399
  308 CONTINUE
      PHIA=175.D0/DEG
      GO TO 399
  309 CONTINUE
      GO TO 399
  310 CONTINUE
      GO TO 399
  311 CONTINUE
      GO TO 399
  312 CONTINUE
      GO TO 399
  313 CONTINUE
      GO TO 399
  314 CONTINUE
      GO TO 399
  315 CONTINUE
      GO TO 399
```

```
  316   CONTINUE
        GO TO 399
  317   CONTINUE
        GO TO 399
  318   CONTINUE
        GO TO 399
  319   CONTINUE
        GO TO 399
  320   CONTINUE
        GO TO 399
  399   CONTINUE
        PRINT 101
  101   FORMAT('1')
C
        CALL INDAT1
C
        DO 200 NX=1,NXS
        XS=XSV(NX)
C  (X0,Y0,Z0) IS THE POINT AT WHICH FLUX AND DENSITY ARE COMPUTED.
C  THE NORMAL TO THE SURFACE AT (X0,Y0,Z0) IS PARALLEL TO Y-AXIS.
        X0=XS
        Y0=A0
        Z0=0.
        DO 20 NS=NS1,NS2
        FLUXC(NS)=0.
        FLXU2C(NS)=0.
        OMEGA(NS)=0.
        DSUMAX(NS)=0.
        IQTOT(NS)=0
        ISHAD(NS)=0.
        TMAX(NS)=-1.D 44
        ETAKMX(NS)=-1.D 44
        PHIMAX(NS)=-1.D 44
        PHIFMX(NS)=-1.D 44
        WMAX(NS)=-1.D 44
        PSIMAX(NS)=-1.D 44
        ETAMAX(NS)=-1.D 44
        RFMAX(NS)=-1.D 44
        EMMAX(NS)=-1.D 44
        FMAX(NS)=-1.D 44
   20   CONTINUE
        RN=RMIN
        APF=A0-0.5D0*DR0*SPSIF
        NR=0
    1   NR=NR+1
        DR=DR0
        DR=DR0*(APF/A0)
C       DR=DR0*(1.D0+0.4D0*DR0/XS)**NR
        RF=RN+DR/2.D0
        APF=A0+RF*SPSIF
        PHISOF=DACOS(A0/APF)
C       DPHI0=0.1D0
C       NPHI=PHISOF/DPHI0+2
        DPHI=PHISOF/DBLE(NPHI)
        DO 21 NS=NS1,NS2
        DSUMF(NS)=0.
        DSUMU2(NS)=0.
        DSUMD(NS)=0.
   21   CONTINUE
        DOMEGR=0.
        DO 2 NP=1,NPHI
        DO 2 IPAR=1,2
        PHIF=(DBLE(NP)-0.5D0)*DPHI
        IF(IPAR.EQ.2) PHIF=-PHIF
C
        CALL FLUX
C
        CROSS1=OMEGY
        CROSS2=(SPSIF)*(-OMEGX)+(-CPSIF*CPHIF)*(-OMEGY)+
     1        (-CPSIF*SPHIF)*(-OMEGZ)
        IF(CROSS1.LE.0.)
     1CALL SOF('DIRECTION COSINE OF SURFACE NORMAL SHOULD BE POSITIVE')
```

```
      IF(CROSS2.LE.0.)
     1CALL SOF('NORMAL TO LIMITING CONE HAS NEGATIVE PROJECTION ON LINE-
     1OF-SIGHT')
      DOMEGA=CROSS2*DPHI*APF*DR/DIST**2
      DOMEGR=DOMEGR+DOMEGA
      DO 24 NS=NS1,NS2
      DSUMF(NS)=DSUMF(NS)+DOMEGA*QFC(NS)*CROSS1
      DSUMU2(NS)=DSUMU2(NS)+DOMEGA*QU2C(NS)*CROSS1
      IF(DSUMAX(NS).GT.DOMEGA*QFC(NS)*CROSS1) GO TO 24
      DSUMAX(NS)=DOMEGA*QFC(NS)*CROSS1
      TMAX(NS)=TEXT(NS)
      ETAKMX(NS)=ETAKXT(NS)
      PHIMAX(NS)=PHIEXT(NS)*DEG
      PHIFMX(NS)=PHIF*DEG
      WMAX(NS)=WEXT(NS)*DEG
      PSIMAX(NS)=PSIEXT(NS)*DEG
      ETAMAX(NS)=ETAEXT(NS)
      RFMAX(NS)=RF
      EMMAX(NS)=EMEXT(NS)
      FMAX(NS)=QFC(NS)*XC(NS)*Q0
   24 CONTINUE
    2 CONTINUE
      DO 26 NS=NS1,NS2
      FLUXC(NS)=FLUXC(NS)+DSUMF(NS)
      FLXU2C(NS)=FLXU2C(NS)+DSUMU2(NS)
      OMEGA(NS)=OMEGA(NS)+DOMEGR
   26 CONTINUE
      RN=RN+DR
      IF(NR.LE.2) GO TO 1
      IF(NR.GT.99) GO TO 10
      DO 27 NS=NS1,NS2
      IF(FLUXC(NS).EQ.0.) GO TO 27
      ERR=(DSUMF(NS)/FLUXC(NS))/DOMEGR
      IF(ERR.GT.EPSR) GO TO 28
   27 CONTINUE
      GO TO 10
   28 CONTINUE
      GO TO 1
   10 CONTINUE
      DO 31 NS=NS1,NS2
      FLUXC(NS)=XC(NS)*FLUXC(NS)*Q0
      OMEGA(NS)=OMEGA(NS)/(2.D0*PAI*DCOS(PSIF/2.D0)**2)
      FLXU2C(NS)=XC(NS)*FLXU2C(NS)*Q0
      URMSC(NS)=0.
      IF(FLUXC(NS).EQ.0.) GO TO 31
      URMSC(NS)=DSQRT(FLXU2C(NS)/FLUXC(NS))
C  AVERAGE EM  (SEE FETA)
      URMSC(NS)=       FLXU2C(NS)/FLUXC(NS)
   31 CONTINUE
      PRINT 11,NX,NR,XS,RF,DR,PHISOF*DEG
   11 FORMAT(///1X,'NX,NR,XS,RF,DR,PHISOF=',2I4,3D13.4,F8.4,
     1        3X,'FLUX AND EXTREMA VALUES, ALL SPECIES:'/)
      PRINT 12
   12 FORMAT(/1X,' NAME ',' IQTOT',' ISHAD',
     1            '   FMAX    ','   OMEGA','     TMAX',
     2            '  ETAKMX','  ETAMAX','  PSIMAX',
     3            '   EMMAX','   RFMAX',' PI-WMAX',
     4            '   URMSC','  FLUXC    / LOG'/)
      DO 14 NS=NS1,NS2
      DLF=0.
      IF(FLUXC(NS).NE.0)
     1DLF=DLOG10(FLUXC(NS))+100.D0+1.D-11
      IDLF=DLF
      DLF=DLF-DBLE(IDLF)
      PRINT 13,XNAME(NS),IQTOT(NS),ISHAD(NS),FMAX(NS),OMEGA(NS),
     1                               TMAX(NS),ETAKMX(NS),ETAMAX(NS),
     2                               PSIMAX(NS),EMMAX(NS),RFMAX(NS),
     3                               180.D0-WMAX(NS),URMSC(NS),
     4                               FLUXC(NS),DLF
   13 FORMAT(1X,A6,2I6,D10.3,4F8.4,4F8.1,F8.2,D10.3,'/',F4.2)
   14 CONTINUE
  200 CONTINUE
```

```
      PRINT 102
  102 FORMAT(///1X,'END  RING  RUN',///)
  300 CONTINUE
      STOP
      END
      SUBROUTINE INIDAT
      IMPLICIT REAL*8(A-H,O-Z)
      REAL*8 LAMDA0,LAMDA1
      CHARACTER*8 XNAME,XNAMED
      COMMON /GAMA/G,G1,G2,G3,G4,G5,G6,G7,G8,G9,G10,G11,G12,G13,G14,G15,
     1             G16,G17,G18,G19,G20
      COMMON /PAR/C0,EN0,EM1,D,SIGMA,TLIM,DR0,EL0,Q0,T0,FACT,ALOGF,
     1            DPSI0,DTMAX,DETA0,ETALIM,XSI,XSF
      COMMON /NPAR/NPHI,IPAR,NP,NR,NX,NXS,NS,NSPEC,NS1,NS2,NTAU0,NETA0,
     1             NAMB,NCASE,ICASE,IFAN
      COMMON /GEOM/APF,PAI,PAI2,W,SW,CW,BETA,SBETA,CBETA,PSI1,SPSI1,
     1             CPSI1,PSIF,SPSIF,CPSIF,TPSIF,AK,SK,CK,A0,RF,XF,YF,ZF,
     2             PHISOF,PHIF,SPHIF,CPHIF,DYMIN,RMIN,XS,DIST,X0,Y0,Z0,
     3             DY0,DEG,PSIN,ST1,CT1,OMEGX,OMEGY,OMEGZ,XSV(21)
      COMMON /EPSIL/EPSETA,EPST,EPSR
      COMMON /EXTREM/TEXT(5),ETAEXT(5),ETAKXT(5),PHIEXT(5),
     1               PSIEXT(5),EMEXT(5),FEXT(5),WEXT(5),
     2               TMAX(5),ETAKMX(5),ETAMAX(5),PSIMAX(5),
     3               EMMAX(5),FMAX(5),
     4               RFMAX(5),PHIFMX(5),PHIMAX(5),WMAX(5)
      COMMON /COUNTS/ICONTC,ICONTT,ICNTOT,ICNTMX,IQTOT(5),ISHAD(5)
      COMMON /SPEC/WAV,XC(5),WC(5),WRC(5),XNAME(5),QFC(5),QDC(5),
     1             QU2C(5),FLUXC(5),OMEGA(5),FLXU2C(5),URMSC(5)
      COMMON /AMBIEN/ENA,UA,PSIA,PHIA,HA(3),WA(3),
     1               UAX,UAY,UAZ,AA,BA,CA,RA,XA,YA,ZA,SHADOW
      COMMON /POINT/XP,YP,XCOR,YCOR
      LOGICAL SHADOW
      DIMENSION XCD(5),WCD(5),XNAMED(5)
      DATA XCD/.091D0,.091D0,.104D0,.135D0,.579D0/
      DATA WCD/1.00D0,20.0D0,2.00D0,21.0D0,4.00D0/
      DATA XNAMED/'   H    ','   HF   ','   H2   ','   DF   ','   HE   '/
      DATA IFIRST/0/
      IFAN=2
      PAI=4.D0*DATAN(1.D0)
      PAI2=PAI/2.D0
      DEG=180.D0/PAI
      AR=8.3143D3
      AV=6.022D 26
C  OMEGAC=0.5 IS FOR HARD SPHERE COLLISIONS,
C  AN AVERAGE RECOMMENDED VALUE IS ABOUT OMEGAC=0.75
      OMEGAC=0.5D0
      NSPEC=5
      NS1=2
      NS2=2
      DO 51 NS=1,NSPEC
      XC(NS)=XCD(NS)
      WC(NS)=WCD(NS)
      XNAME(NS)=XNAMED(NS)
   51 CONTINUE
C  COMBINE HF AND DF MOLE FRACTIONS INTO HF FRACTION
      XC(2)=XC(2)+XC(4)
      XC(4)=0.
C
      A0=2.5D0
      EM1=4.D0
      RHO0=0.0075D0
      T0=1400.D0
      G=1.54D0
      D=2.5D-10
      NXS=1
      XSI=1.0D0
      XSF=10.D0
C  AMBIENT AIR
      ENA=1.00D 16
      UA=8.D 3
      NAMB=3
      WA(1)=28.D0
```

```
      WA(2)=32.D0                                                        AMB0289
      WA(3)=16.D0                                                        AMB0290
      HA(1)=1.D0                                                         AMB0291
      HA(2)=0.                                                           AMB0292
      HA(3)=0.                                                           AMB0293
      PSIA=20.D0/DEG                                                     AMB0294
      PHIA=0.00D0/DEG                                                    AMB0295
C  INTEGRATION PARAMETERS                                                AMB0296
      NPHI=6                                                             AMB0297
      NTAU0=4                                                            AMB0298
      NETA0=4                                                            AMB0299
      ICNTMX=100                                                         AMB0300
      RMIN=0.                                                            AMB0301
      DR0=0.10D0                                                         AMB0302
      DPSI0=0.20D0                                                       AMB0303
      DTMAX=1.0D0                                                        AMB0304
      DETA0=0.50D0                                                       AMB0305
      ETALIM=10.D0                                                       AMB0306
      EPST=0.5D0                                                         AMB0307
      EPSR=0.3D0                                                         AMB0308
      FACT=1.D 20                                                        AMB0309
      RETURN                                                             AMB0310
C*********************************************************************** AMB0311
C  COMPUTATION OF DATA-DEPENDENT PARAMETERS                              AMB0312
C*********************************************************************** AMB0313
      ENTRY INDAT1                                                       AMB0314
C*********************************************************************** AMB0315
      ALOGF=DLOG(FACT)                                                   AMB0316
      WAV=0.                                                             AMB0317
      DO 52 NS=1,NSPEC                                                   AMB0318
      WAV=WAV+XC(NS)*WC(NS)                                              AMB0319
 52   CONTINUE                                                           AMB0320
      DO 53 NS=1,NSPEC                                                   AMB0321
      WRC(NS)=WC(NS)/WAV                                                 AMB0322
 53   CONTINUE                                                           AMB0323
      SIGMA=PAI*D**2                                                     AMB0324
      EN0=RHO0*AV/WAV                                                    AMB0325
      C0=DSQRT(G*AR*T0/WAV)                                              AMB0326
      XSV(1)=XSI                                                         AMB0327
      IF(NXS.EQ.1) GO TO 12                                              AMB0328
      DXL=(DLOG(XSF)-DLOG(XSI))/(DBLE(NXS)-1.D0)                         AMB0329
      XLI=DLOG(XSI)                                                      AMB0330
      DO 11 NX=2,NXS                                                     AMB0331
      XSV(NX)=DEXP(XLI+(DBLE(NX)-1.D0)*DXL)                              AMB0332
 11   CONTINUE                                                           AMB0333
 12   CONTINUE                                                           AMB0334
      G1=(G-1.D0)/2.D0                                                   AMB0335
      G2=(G+1.D0)/(2.D0*(G-1.D0))                                        AMB0336
      G3=G/2.D0                                                          AMB0337
      G4=(G+1.D0)/(G-1.D0)                                               AMB0338
      G5=DSQRT((G+1.D0)/(G-1.D0))                                        AMB0339
      G6=1.D0/(G-1.D0)                                                   AMB0340
      G7=2.D0/(G+1.D0)                                                   AMB0341
      G8=(0.5D0*(G+1.D0)**2/(G-1.D0))**(1.D0/(G+1.D0))*                  AMB0342
     1   ((G+1.D0)/(G-1.D0))**((G-1.D0)/(G+1.D0))                        AMB0343
      G9=(G+3.D0)/(2.D0*(G-1.D0))                                        AMB0344
      G10=(7.D0-3.D0*G)/(2.D0*(G-1.D0))                                  AMB0345
      G11=(5.D0-3.D0*G)/(2.D0*(G-1.D0))                                  AMB0346
      G13=(2.D0-G)/(2.D0*(G-1.D0))                                       AMB0347
      G14=G/(2.D0*(G-1.D0))                                              AMB0348
      G15=(G+1.D0)/(3.D0-G)                                              AMB0349
      ZETA1=G5*DATAN(DSQRT(EM1**2-1.D0)/G5)                              AMB0350
      AMU1=DASIN(1.D0/EM1)                                               AMB0351
      PSI1=PAI2+AMU1                                                     AMB0352
      SPSI1=DSIN(PSI1)                                                   AMB0353
      CPSI1=DCOS(PSI1)                                                   AMB0354
      PSIF=PAI2+AMU1+ZETA1-G5*PAI2                                       AMB0355
      SPSIF=DSIN(PSIF)                                                   AMB0356
      CPSIF=DCOS(PSIF)                                                   AMB0357
      TPSIF=DTAN(PSIF)                                                   AMB0358
      TETA1=PSI1-AMU1                                                    AMB0359
      ST1=DSIN(TETA1)                                                    AMB0360
```

```
      CT1=DCOS(TETA1)
      Q0=ENA*UA
      LAMDA0=1.D0/(DSQRT(2.D0)*SIGMA*EN0)
      LAMDA1=LAMDA0*(1.D0+G1*EM1**2)**(G6-OMEGAC+0.5D0)
      AA=DCOS(PSIA)
      BA=DSIN(PSIA)*DCOS(PHIA)
      CA=DSIN(PSIA)*DSIN(PHIA)
      UAX=-UA*AA
      UAY=-UA*BA
      UAZ=-UA*CA
      XCOR=0.
      YCOR=A0
C
      PRINT 201,NSPEC,XNAME
  201 FORMAT(/1X,'SPECIES DATA   NSPEC=',I3/
     1        1X,'SPECIES NAMES     ',11(2X,A6,2X))
      PRINT 202,XC
  202 FORMAT( 1X,'MOLE FRACTION XC=',11(F8.4,2X))
      PRINT 203,WC
  203 FORMAT( 1X,'MOL. WEIGHT   WC=',11(F8.4,2X))
      PRINT 21,AR,AV,WAV,G,RHO0,T0,EN0,C0,D
  21  FORMAT(/1X,'THERMODYNAMIC DATA'/
     1        1X,'AR,AV,WAV,GAMMA=',2X,2D14.5,2F9.3/
     2        1X,'RHO0,T0,EN0,C0,D=',D12.4,F8.0,D13.5,2D12.4)
      PRINT 22,EM1,PSI1*DEG,PSIF*DEG,
     1         A0,LAMDA0,LAMDA1
  22  FORMAT(/1X,'FLOW AND GEOMETRY DATA'/
     1        1X,'EM1,PSI1,PSIF=',3F9.3/
     2        1X,'A0,LAMDA0,LAMDA1=',F9.3,2D13.4)
      PRINT 23,DPSI0,DTMAX,DETA0,ETALIM,DR0,RMIN,
     1         EPST,EPSR,
     2         NPHI,NTAU0,NETA0
  23  FORMAT(/1X,'INTEGRATION DATA'/
     1        1X,'DPSI0,DTMAX,DETA0,ETALIM=',4F9.4/
     2        1X,'DR0,RMIN,=',2D13.4/
     3        1X,'EPST,EPSR=',2D12.3/
     4        1X,'NPHI,NTAU0,NETA0=',3I6)
      PRINT 24,ENA,UA,PSIA*DEG,PHIA*DEG
  24  FORMAT(/1X,'ABBREVIATED AIR DATA'/
     1        1X,'ENA,UA=',2D13.4/
     2        1X,'PSIA,PHIA=',2F9.1)
      GO TO (251,252), IFAN

  251 CONTINUE
      PRINT 2510, IFAN
 2510 FORMAT(/1X,'RING-FAN APPROXIMATED AS PLANAR.   IFAN=',I4)
      GO TO 250
  252 CONTINUE
      PRINT 2520, IFAN
 2520 FORMAT(/1X,'RING-FAN APPROXIMATED BY MATCHED APPROXIMATION.',
     1        4X,'IFAN=',I4)
  250 CONTINUE
      PRINT 29
  29  FORMAT(///1X,'END  DATA'///)
      IF(IFIRST.EQ.0.AND.IFAN.EQ.2)
     1CALL HMSET
      IF(IFAN.EQ.2) IFIRST=IFIRST+1
      RETURN
      END
C$OPTIONS LIST
      SUBROUTINE SOF(ISTOP)
      IMPLICIT REAL*8(A-H,O-Z)
      CHARACTER*4 ISTOP(1)
      COMMON /GAMA/G,G1,G2,G3,G4,G5,G6,G7,G8,G9,G10,G11,G12,G13,G14,G15,
     1              G16,G17,G18,G19,G20
      COMMON /PAR/C0,EN0,EM1,D,SIGMA,TLIM,DR0,EL0,Q0,T0,FACT,ALOGF,
     1             DPSI0,DTMAX,DETA0,ETALIM,XSI,XSF
      COMMON /NPAR/NPHI,IPAR,NP,NR,NX,NXS,NS,NSPEC,NS1,NS2,NTAU0,NETA0,
     1              NAMB,NCASE,ICASE,IFAN
      COMMON /GEOM/APF,PAI,PAI2,W,SW,CW,BETA,SBETA,CBETA,PSI1,SPSI1,
     1              CPSI1,PSIF,SPSIF,CPSIF,TPSIF,AK,SK,CK,A0,RF,XF,YF,ZF,
     2              PHISOF,PHIF,SPHIF,CPHIF,DYMIN,RMIN,XS,DIST,X0,Y0,Z0,
```

```
     3              DY0,DEG,PSIN,ST1,CT1,OMEGX,OMEGY,OMEGZ,XSV(21)
      COMMON /EPSIL/EPSETA,EPST,EPSR
      COMMON /EXTREM/TEXT(5),ETAEXT(5),ETAKXT(5),PHIEXT(5),
     1                 PSIEXT(5),EMEXT(5),FEXT(5),WEXT(5),
     2                 TMAX(5),ETAKMX(5),ETAMAX(5),PSIMAX(5),
     3                 EMMAX(5),FMAX(5),
     4                 RFMAX(5),PHIFMX(5),PHIMAX(5),WMAX(5)
      COMMON /SOFPR/C,DSUMF,DSUMD,T,ETA,DETA,SUM,DSUM,SUMU,DSUMU
      COMMON /SUMS/SUMF(5),SUMD(5),SUMU2(5)
      COMMON /COUNTS/ICONTC,ICONTT,ICNTOT,ICNTMX,IQTOT(5),ISHAD(5)
      COMMON /SPEC/WAV,XC(5),WC(5),WRC(5),XNAME(5),QFC(5),QDC(5),
     1              QU2C(5),FLUXC(5),OMEGA(5),FLXU2C(5),URMSC(5)
      PRINT 1,ISTOP
 1    FORMAT(///1X,2H**,2X,30A4,2X,2H**,///)
      PRINT 71,NS,NP,NR,NX,ICONTC,ICONTT
 71   FORMAT(1X,'NS,NP,NR,NX,ICONTC,ICONTT=',6I6/)
      IF(NS.GT.NSPEC) NS=1
      PRINT 72,RF,PHIF*DEG,PHISOF*DEG,W*DEG,BETA*DEG
 72   FORMAT(/1X,'RF,PHIF,PHISOF,W,BETA=',D14.5,4F10.3/)
      PRINT 73,C,T,TLIM,ETA
 73   FORMAT(/1X,'C,T,TLIM,ETA=',4D14.5/)
      PRINT 74,DSUM,SUM,DSUMF,SUMF(NS),SUMD(NS),QDC(NS),QFC(NS),
     1         FLUXC(NS),OMEGA(NS)
 74   FORMAT(1X,'DSUM,SUM,DSUMF,SUMF(NS),SUMD(NS)=',5D14.5/
     1       1X,'QDC(NS),QFC(NS),FLUXC(NS),OMEGA(NS)=',4D14.5/)
      XX=-1.D0
      YY=DSQRT(XX)+1.D0
      STOP
      END
      SUBROUTINE FLUX
      IMPLICIT REAL*8(A-H,O-Z)
      COMMON /GAMA/G,G1,G2,G3,G4,G5,G6,G7,G8,G9,G10,G11,G12,G13,G14,G15,
     1              G16,G17,G18,G19,G20
      COMMON /PAR/C0,EN0,EM1,D,SIGMA,TLIM,DR0,EL0,Q0,T0,FACT,ALOGF,
     1            DPSI0,DTMAX,DETA0,ETALIM,XSI,XSF
      COMMON /NPAR/NPHI,IPAR,NP,NR,NX,NXS,NS,NSPEC,NS1,NS2,NTAU0,NETA0,
     1              NAMB,NCASE,ICASE,IFAN
      COMMON /GEOM/APF,PAI,PAI2,W,SW,CW,BETA,SBETA,CBETA,PSI1,SPSI1,
     1              CPSI1,PSIF,SPSIF,CPSIF,TPSIF,AK,SK,CK,A0,RF,XF,YF,ZF,
     2              PHISOF,PHIF,SPHIF,CPHIF,DYMIN,RMIN,XS,DIST,X0,Y0,Z0,
     3              DY0,DEG,PSIN,ST1,CT1,OMEGX,OMEGY,OMEGZ,XSV(21)
      COMMON /EPSIL/EPSETA,EPST,EPSR
      COMMON /EXTREM/TEXT(5),ETAEXT(5),ETAKXT(5),PHIEXT(5),
     1                 PSIEXT(5),EMEXT(5),FEXT(5),WEXT(5),
     2                 TMAX(5),ETAKMX(5),ETAMAX(5),PSIMAX(5),
     3                 EMMAX(5),FMAX(5),
     4                 RFMAX(5),PHIFMX(5),PHIMAX(5),WMAX(5)
      COMMON /SOFPR/C,DSUMF,DSUMD,T,ETA,DETA,SUM,DSUM,SUMU,DSUMU
      COMMON /COUNTS/ICONTC,ICONTT,ICNTOT,ICNTMX,IQTOT(5),ISHAD(5)
      COMMON /SPEC/WAV,XC(5),WC(5),WRC(5),XNAME(5),QFC(5),QDC(5),
     1              QU2C(5),FLUXC(5),OMEGA(5),FLXU2C(5),URMSC(5)
      COMMON /SUMS/SUMF(5),SUMD(5),SUMU2(5)
      EL0=SIGMA*RF*EN0
      IF(Z0.NE.0.)
     1CALL SOF('THE SCHEME HERE IS NOT WRITTEN FOR Z0.NE.0.')
      YY0=(Y0-A0)/X0
      PCHECK=DATAN(YY0)
      IF(PCHECK.GT.PSIF-1.D-4.OR.PCHECK.LT.-1.D-4)
     1CALL SOF('FLUX RECEIVING POINT WITHIN FAN OR WITHIN SPACECRAFT')
      SPHIF=DSIN(PHIF)
      CPHIF=DCOS(PHIF)
      XF=RF*CPSIF
      YF=APF*CPHIF
      ZF=APF*SPHIF
      TBETA=ZF/(YF-Y0)
      BETA=DATAN(TBETA)
      IF(DABS(BETA).GT.PAI2) CALL SOF('BETA.GT.PAI/2')
      SBETA=DSIN(BETA)
      CBETA=DCOS(BETA)
      DIST=DSQRT((XF-X0)**2+(YF-Y0)**2+(ZF-Z0)**2)
      CW=(XF-X0)/DIST
      SW=DSQRT(1.D0-CW**2)
```

```
      W=PAI2-DATAN(CW/SW)
      OMEGX=CW
      OMEGY=SW*CBETA
      OMEGZ=SW*SBETA
      CALL LIMIT
C
      DO 20 NS=NS1,NS2
      SUMF(NS)=0.
      SUMU2(NS)=0.
      SUMD(NS)=0.
      FEXT(NS)=0.
      CALL SUMT
      SUMF(NS)=SUM
      SUMU2(NS)=SUMU
      QFC(NS)=SUMF(NS)/FACT
      QU2C(NS)=SUMU2(NS)/FACT
      FEXT(NS)=FEXT(NS)/FACT
      CALL FAN(TEXT(NS),PSIEXT(NS),PHIEXT(NS))
      IF(PSIEXT(NS).LT.PSIF-1.D-10) CALL SOF('PSIEXT(NS).LT.PSIF')
      IF(PSIEXT(NS).GT.PSI1) PSIEXT(NS)=PSI1
      PSI0=PSIEXT(NS)
      T=TEXT(NS)
      CALL MATCH(T,PSI0,EM,TETA)
      EMEXT(NS)=EM
      WEXT(NS)=W
      IQTOT(NS)=IQTOT(NS)+ICONTT
   20 CONTINUE
      RETURN
      END
      SUBROUTINE LIMIT
      IMPLICIT REAL*8(A-H,O-Z)
      COMMON /GAMA/G,G1,G2,G3,G4,G5,G6,G7,G8,G9,G10,G11,G12,G13,G14,G15,
     1             G16,G17,G18,G19,G20
      COMMON /PAR/C0,EN0,EM1,D,SIGMA,TLIM,DR0,EL0,Q0,T0,FACT,ALOGF,
     1            DPSI0,DTMAX,DETA0,ETALIM,XSI,XSF
      COMMON /NPAR/NPHI,IPAR,NP,NR,NX,NXS,NS,NSPEC,NS1,NS2,NTAU0,NETA0,
     1             NAMB,NCASE,ICASE,IFAN
      COMMON /GEOM/APF,PAI,PAI2,W,SW,CW,BETA,SBETA,CBETA,PSI1,SPSI1,
     1             CPSI1,PSIF,SPSIF,CPSIF,TPSIF,AK,SK,CK,A0,RF,XF,YF,ZF,
     2             PHISOF,PHIF,SPHIF,CPHIF,DYMIN,RMIN,XS,DIST,X0,Y0,Z0,
     3             DY0,DEG,PSIN,ST1,CT1,OMEGX,OMEGY,OMEGZ,XSV(21)
      COMMON /EPSIL/EPSETA,EPST,EPSR
      COMMON /EXTREM/TEXT(5),ETAEXT(5),ETAKXT(5),PHIEXT(5),
     1               PSIEXT(5),EMEXT(5),FEXT(5),WEXT(5),
     2               TMAX(5),ETAKMX(5),ETAMAX(5),PSIMAX(5),
     3               EMMAX(5),FMAX(5),
     4               RFMAX(5),PHIFMX(5),PHIMAX(5),WMAX(5)
      COMMON /SPEC/WAV,XC(5),WC(5),WRC(5),XNAME(5),QFC(5),QDC(5),
     1             QU2C(5),FLUXC(5),OMEGA(5),FLXU2C(5),URMSC(5)
      AAA=(CW/CPSI1)**2-1.D0
      IF(AAA.LT.1.D-10) GO TO 1
      TPSI1=SPSI1/CPSI1
      AP1=A0+XF*TPSI1
      BBB=2.D0*(AP1*CW*TPSI1-SW*APF*(CBETA*CPHIF+SBETA*SPHIF))
      CCC=AP1**2-APF**2
      DDD=BBB**2-4.D0*AAA*CCC
      TLIM=(-BBB+DSQRT(DDD))/(2.D0*AAA)
      TLIM=TLIM/RF
      RETURN
    1 CONTINUE
      TLIM=1.D 55
      RETURN
      END
      SUBROUTINE SUMT
      IMPLICIT REAL*8(A-H,O-Z)
      COMMON /GAMA/G,G1,G2,G3,G4,G5,G6,G7,G8,G9,G10,G11,G12,G13,G14,G15,
     1             G16,G17,G18,G19,G20
      COMMON /PAR/C0,EN0,EM1,D,SIGMA,TLIM,DR0,EL0,Q0,T0,FACT,ALOGF,
     1            DPSI0,DTMAX,DETA0,ETALIM,XSI,XSF
      COMMON /NPAR/NPHI,IPAR,NP,NR,NX,NXS,NS,NSPEC,NS1,NS2,NTAU0,NETA0,
     1             NAMB,NCASE,ICASE,IFAN
      COMMON /GEOM/APF,PAI,PAI2,W,SW,CW,BETA,SBETA,CBETA,PSI1,SPSI1,
```

```
     1              CPSI1,PSIF,SPSIF,CPSIF,TPSIF,AK,SK,CK,A0,RF,XF,YF,ZF,
     2              PHISOF,PHIF,SPHIF,CPHIF,DYMIN,RMIN,XS,DIST,X0,Y0,Z0,
     3              DY0,DEG,PSIN,ST1,CT1,OMEGX,OMEGY,OMEGZ,XSV(21)
      COMMON /EPSIL/EPSETA,EPST,EPSR
      COMMON /EXTREM/TEXT(5),ETAEXT(5),ETAKXT(5),PHIEXT(5),
     1               PSIEXT(5),EMEXT(5),FEXT(5),WEXT(5),
     2               TMAX(5),ETAKMX(5),ETAMAX(5),PSIMAX(5),
     3               EMMAX(5),FMAX(5),
     4               RFMAX(5),PHIFMX(5),PHIMAX(5),WMAX(5)
      COMMON /SOFPR/CC,DSUMF,DSUMD,T,ETA,DETA,SUM,DSUM,SUMU,DSUMU
      COMMON /COUNTS/ICONTC,ICONTT,ICNTOT,ICNTMX,IQTOT(5),ISHAD(5)
      COMMON /SPEC/WAV,XC(5),WC(5),WRC(5),XNAME(5),QFC(5),QDC(5),
     1            QU2C(5),FLUXC(5),OMEGA(5),FLXU2C(5),URMSC(5)
      COMMON /SUMS/SUMF(5),SUMD(5),SUMU2(5)
C  INTEGRATION OF FLUX ARRIVING ALONG A SINGLE RAY
      DT=DPSI0
      PSIN=PSIF
      ETA1=0.
      ETA3=0.
      FETA4=0.
      FETAU4=0.
      T=0.
      SUM=0.
      SUMU=0.
      ICONTT=0
    1 ICONTT=ICONTT+1
      PSIL=PSIN
      DT2=DT/2.D0
      DT6=DT/6.D0
      T1=T+DT2
      T2=T+DT
      FETA1=FETA4
      FETAU1=FETAU4
      CALL PATHK(T1,ETAK1)
      CALL FETA(T1,ETA1,ETAK1,GT2,FETA2,FETAU2)
      FETA3=FETA2
      FETAU3=FETAU2
      CALL PATHK(T2,ETAK3)
      CALL FETA(T2,ETA3,ETAK3,GT4,FETA4,FETAU4)
      DETA=DT*GT4
      DSUM=DT6*(FETA1+2.D0*(FETA2+FETA3)+FETA4)
      DSUMU=DT6*(FETAU1+2.D0*(FETAU2+FETAU3)+FETAU4)
      T=T+DT
      ETA=ETA3
      ETAK=ETAK3
      SUM=SUM+DSUM
      SUMU=SUMU+DSUMU
      IF(FEXT(NS).GT.FETA4) GO TO 10
      FEXT(NS)=FETA4
      TEXT(NS)=T
      ETAEXT(NS)=ETA
      ETAKXT(NS)=ETAK
   10 CONTINUE
C  STEP CONTROL (DT)
      CALL FAN(T,PSI,PHI)
      IF(PSI.LT.PSIF-1.D-10) CALL SOF('PSI.LT.PSIF')
      IF(PSI.GT.PSI1) PSI=PSI1
      PSIN=PSI
      DPSI=PSIN-PSIL
      DTP=DT*(DPSI0/(DPSI+1.D-10))
      DTE=DT*(DETA0/(DETA+1.D-10))
      DT1=1.2D0*DT
      DT=DMIN1(DTP,DTE,DT1,DTMAX)
      IF(DT.LE.0.) CALL SOF('COMPUTED DT NEGATIVE')
   15 CONTINUE
      IF(IPAR.LT.1)
     1PRINT 111,NR,NP,T,PSI*DEG,PHI*DEG,ETA,ETAK,SUM,DSUM/(SUM+1.D-20)
  111   FORMAT(1X,'NR,NP,T,PSI,PHI=',2I3,3D12.3/
     1         1X,'ETA,ETAK,SUM,ERRR=',4D12.3)
      IF(ICONTT.GT.ICNTMX)
     1CALL SOF('ICONTT TOO LARGE')
      IF(ICONTT.LE.2) GO TO 1
```

```
      IF(ETA+ETAK.GT.ETALIM) GO TO 100
      IF(T.GT.50.D0 .OR. T*RF.GT.A0) GO TO 100
      IF(SUM.EQ.0.) GO TO 1
      ERR=(DSUM/SUM)/DT
      IF(ERR.GT.EPST) GO TO 1
  100 CONTINUE
      SUM=SUM*EL0
      SUMU=SUMU*EL0
      RETURN
      END
      SUBROUTINE FETA(T,ETAIK,ETAK,GT,FET,FETU2)
      IMPLICIT REAL*8(A-H,O-Z)
      REAL*8 MU1,MU2
      COMMON /GAMA/G,G1,G2,G3,G4,G5,G6,G7,G8,G9,G10,G11,G12,G13,G14,G15,
     1             G16,G17,G18,G19,G20
      COMMON /PAR/C0,EN0,EM1,D,SIGMA,TLIM,DR0,EL0,Q0,T0,FACT,ALOGF,
     1            DPSI0,DTMAX,DETA0,ETALIM,XSI,XSF
      COMMON /NPAR/NPHI,IPAR,NP,NR,NX,NXS,NS,NSPEC,NS1,NS2,NTAU0,NETA0,
     1             NAMB,NCASE,ICASE,IFAN
      COMMON /GEOM/APF,PAI,PAI2,W,SW,CW,BETA,SBETA,CBETA,PSI1,SPSI1,
     1             CPSI1,PSIF,SPSIF,CPSIF,TPSIF,AK,SK,CK,A0,RF,XF,YF,ZF,
     2             PHISOF,PHIF,SPHIF,CPHIF,DYMIN,RMIN,XS,DIST,X0,Y0,Z0,
     3             DY0,DEG,PSIN,ST1,CT1,OMEGX,OMEGY,OMEGZ,XSV(21)
      COMMON /EPSIL/EPSETA,EPST,EPSR
      COMMON /EXTREM/TEXT(5),ETAEXT(5),ETAKXT(5),PHIEXT(5),
     1               PSIEXT(5),EMEXT(5),FEXT(5),WEXT(5),
     2               TMAX(5),ETAKMX(5),ETAMAX(5),PSIMAX(5),
     3               EMMAX(5),FMAX(5),
     4               RFMAX(5),PHIFMX(5),PHIMAX(5),WMAX(5)
      COMMON /SPEC/WAV,XC(5),WC(5),WRC(5),XNAME(5),QFC(5),QDC(5),
     1             QU2C(5),FLUXC(5),OMEGA(5),FLXU2C(5),URMSC(5)
      COMMON /AMBIEN/ENA,UA,PSIA,PHIA,HA(3),WA(3),
     1               UAX,UAY,UAZ,AA,BA,CA,RA,XA,YA,ZA,SHADOW
      LOGICAL SHADOW
      COMMON /NAGESH/PIK,UIK,UIKX,UIKY,UIKZ
      ETAIK=0.
      IF(SHADOW) GO TO 1
      K=1
      I=NS
      CALL FAN(T,PSI,PHI)
      IF(PSI.LT.PSIF-1.D-10) CALL SOF('PSI.LT.PSIF')
      IF(PSI.GT.PSI1) PSI=PSI1
      PSI0=PSI
      CALL MATCH(T,PSI0,EM,TETA)
      SPSI=DSIN(PSI)
      CPSI=DCOS(PSI)
      SPHI=DSIN(PHI)
      CPHI=DCOS(PHI)
      ST=DSIN(TETA)
      CT=DCOS(TETA)
      GOREM=1.D0+G1*EM**2
      TERMN=GOREM**G6
      U=EM*C0/DSQRT(GOREM)
      UX=U*CT
      UY=U*ST*CPHI
      UZ=U*ST*SPHI
C  COLLISION
      MU1=WC(I)/(WC(I)+WA(K))
      MU2=1.D0-MU1
      UMX=MU1*UX+MU2*UAX
      UMY=MU1*UY+MU2*UAY
      UMZ=MU1*UZ+MU2*UAZ
      DOTUM=OMEGX*UMX+OMEGY*UMY+OMEGZ*UMZ
      URX=UX-UAX
      URY=UY-UAY
      URZ=UZ-UAZ
      UR=DSQRT(URX**2+URY**2+URZ**2)
      DET=DOTUM**2+(MU2*UR)**2-(UMX**2+UMY**2+UMZ**2)
      IF(DET.LT.0.) GO TO 1
      DET1=DSQRT(DET)
      UIK1=-DOTUM+DET1
      UIK2=-DOTUM-DET1
```

```
      IF(UIK2.GT.0.) CALL SOF('DOUBLE COLLISION OPTION NOT PROGRAMMED
     1 YET')
      UIK=UIK1
      IF(UIK.LE.0.) GO TO 1
      UIKX=-OMEGX*UIK
      UIKY=-OMEGY*UIK
      UIKZ=-OMEGZ*UIK
      CDEL=(DOTUM+UIK)/(MU2*UR)
      IF(CDEL.LE.0.) CALL SOF('CDEL NEGATIVE NOT PROGRAMMED YET')
      IF(CDEL-1.D-10.GT.1.D0)
     1CALL SOF('CDEL (COS(DELTA)) CANNOT BE GT.1.')
      PIK=(UIK/(MU2*UR))**2/(4.D0*PAI*CDEL)
      IF (PIK.LT.0.) CALL SOF('PIK.LT.0')
      FET=(UR/UA)*PIK/TERMN
      UREL=DSQRT((UX-UIKX)**2+(UY-UIKY)**2+(UZ-UIKZ)**2)
      GT=EL0*(UREL/UIK)/TERMN
      CALL PATHIK(T,ETAIK)
      POWER=ETAIK+ETAK-ALOGF
      EFACT=0.
      IF(POWER.LT.60.D0)EFACT=DEXP(-POWER)
      FET=FET*EFACT
      FETU2=FET*UIK**2
      IF(EM.LT.0.) CALL SOF('EM.LT.0')
      FETU2=FET*EM
      RETURN
    1 CONTINUE
      FET=0.
      FETU2=0.
      GT=0.
      RETURN
      END
      SUBROUTINE PATHIK(TC,ETAIK)
      IMPLICIT REAL*8(A-H,O-Z)
      REAL*8 MU1,MU2
      COMMON /GAMA/G,G1,G2,G3,G4,G5,G6,G7,G8,G9,G10,G11,G12,G13,G14,G15,
     1             G16,G17,G18,G19,G20
      COMMON /PAR/C0,EN0,EM1,D,SIGMA,TLIM,DR0,EL0,Q0,T0,FACT,ALOGF,
     1            DPSI0,DTMAX,DETA0,ETALIM,XSI,XSF
      COMMON /NPAR/NPHI,IPAR,NP,NR,NX,NXS,NS,NSPEC,NS1,NS2,NTAU0,NETA0,
     1             NAMB,NCASE,ICASE,IFAN
      COMMON /GEOM/APF,PAI,PAI2,W,SW,CW,BETA SBETA,CBETA,PSI1,SPSI1,
     1             CPSI1,PSIF,SPSIF,CPSIF,TPSIF,AK,SK,CK,A0,RF,XF,YF,ZF,
     2             PHISOF,PHIF,SPHIF,CPHIF,DYMIN,RMIN,XS,DIST,X0,Y0,Z0,
     3             DY0,DEG,PSIN,ST1,CT1,OMEGX,OMEGY,OMEGZ,XSV(21)
      COMMON /EPSIL/EPSETA,EPST,EPSR
      COMMON /EXTREM/TEXT(5),ETAEXT(5),ETAKXT(5),PHIEXT(5),
     1               PSIEXT(5),EMEXT(5),FEXT(5),WEXT(5),
     2               TMAX(5),ETAKMX(5),ETAMAX(5),PSIMAX(5),
     3               EMMAX(5),FMAX(5),
     4               RFMAX(5),PHIFMX(5),PHIMAX(5),WMAX(5)
      COMMON /SPEC/WAV,XC(5),WC(5),WRC(5),XNAME(5),QFC(5),QDC(5),
     1             QU2C(5),FLUXC(5),OMEGA(5),FLXU2C(5),URMSC(5)
      COMMON /AMBIEN/ENA,UA,PSIA,PHIA,HA(3),WA(3),
     1               UAX,UAY,UAZ,AA,BA,CA,RA,XA,YA,ZA,SHADOW
      LOGICAL SHADOW
      NETA=NETA0
      DT=TC/DBLE(NETA)
      DT2=DT/2.D0
      DT6=DT/6.D0
      GT4=0.
      T=0.
      ETA=0.
      IT=0
    1 IT=IT+1
      T1=T+DT2
      T2=T+DT
      GT1=GT4
      CALL FT(T1,GT2)
      GT3=GT2
      CALL FT(T2,GT4)
      DETA=DT6*(GT1+2.D0*(GT2+GT3)+GT4)
      T=T+DT
```

```
      ETA=ETA+DETA
      IF(IT.LT.NETA) GO TO 1
      ETAIK=ETA
      RETURN
      END
      SUBROUTINE FT(T,GT)
      IMPLICIT REAL*8(A-H,O-Z)
      REAL*8 MU1,MU2
      COMMON /GAMA/G,G1,G2,G3,G4,G5,G6,G7,G8,G9,G10,G11,G12,G13,G14,G15,
     1          G16,G17,G18,G19,G20
      COMMON /PAR/C0,EN0,EM1,D,SIGMA,TLIM,DR0,EL0,Q0,T0,FACT,ALOGF,
     1         DPSI0,DTMAX,DETA0,ETALIM,XSI,XSF
      COMMON /NPAR/NPHI,IPAR,NP,NR,NX,NXS,NS,NSPEC,NS1,NS2,NTAU0,NETA0,
     1          NAMB,NCASE,ICASE,IFAN
      COMMON /GEOM/APF,PAI,PAI2,W,SW,CW,BETA,SBETA,CBETA,PSI1,SPSI1,
     1          CPSI1,PSIF,SPSIF,CPSIF,TPSIF,AK,SK,CK,A0,RF,XF,YF,ZF,
     2          PHISOF,PHIF,SPHIF,CPHIF,DYMIN,RMIN,XS,DIST,X0,Y0,Z0,
     3          DY0,DEG,PSIN,ST1,CT1,OMEGX,OMEGY,OMEGZ,XSV(21)
      COMMON /EPSIL/EPSETA,EPST,EPSR
      COMMON /EXTREM/TEXT(5),ETAEXT(5),ETAKXT(5),PHIEXT(5),
     1             PSIEXT(5),EMEXT(5),FEXT(5),WEXT(5),
     2             TMAX(5),ETAKMX(5),ETAMAX(5),PSIMAX(5),
     3             EMMAX(5),FMAX(5),
     4             RFMAX(5),PHIFMX(5),PHIMAX(5),WMAX(5)
      COMMON /SPEC/WAV,XC(5),WC(5),WRC(5),XNAME(5),QFC(5),QDC(5),
     1          QU2C(5),FLUXC(5),OMEGA(5),FLXU2C(5),URMSC(5)
      COMMON /AMBIEN/ENA,UA,PSIA,PHIA,HA(3),WA(3),
     1             UAX,UAY,UAZ,AA,BA,CA,RA,XA,YA,ZA,SHADOW
      LOGICAL SHADOW
      COMMON /NAGESH/PIK,UIK,UIKX,UIKY,UIKZ
      K=1
      I=NS
      CALL FAN(T,PSI,PHI)
      IF(PSI.LT.PSIF-1.D-10) CALL SOF('PSI.LT.PSIF')
      IF(PSI.GT.PSI1) PSI=PSI1
      PSI0=PSI
      CALL MATCH(T,PSI0,EM,TETA)
      SPSI=DSIN(PSI)
      CPSI=DCOS(PSI)
      SPHI=DSIN(PHI)
      CPHI=DCOS(PHI)
      ST=DSIN(TETA)
      CT=DCOS(TETA)
      GOREM=1.D0+G1*EM**2
      TERMN=GOREM**G6
      U=EM*C0/DSQRT(GOREM)
      UX=U*CT
      UY=U*ST*CPHI
      UZ=U*ST*SPHI
      UREL=DSQRT((UX-UIKX)**2+(UY-UIKY)**2+(UZ-UIKZ)**2)
      GT=EL0*(UREL/UIK)/TERMN
      RETURN
      END
      SUBROUTINE PATHK(T,ETAK)
      IMPLICIT REAL*8(A-H,O-Z)
      COMMON /GAMA/G,G1,G2,G3,G4,G5,G6,G7,G8,G9,G10,G11,G12,G13,G14,G15,
     1          G16,G17,G18,G19,G20
      COMMON /PAR/C0,EN0,EM1,D,SIGMA,TLIM,DR0,EL0,Q0,T0,FACT,ALOGF,
     1         DPSI0,DTMAX,DETA0,ETALIM,XSI,XSF
      COMMON /NPAR/NPHI,IPAR,NP,NR,NX,NXS,NS,NSPEC,NS1,NS2,NTAU0,NETA0,
     1          NAMB,NCASE,ICASE,IFAN
      COMMON /GEOM/APF,PAI,PAI2,W,SW,CW,BETA,SBETA,CBETA,PSI1,SPSI1,
     1          CPSI1,PSIF,SPSIF,CPSIF,TPSIF,AK,SK,CK,A0,RF,XF,YF,ZF,
     2          PHISOF,PHIF,SPHIF,CPHIF,DYMIN,RMIN,XS,DIST,X0,Y0,Z0,
     3          DY0,DEG,PSIN,ST1,CT1,OMEGX,OMEGY,OMEGZ,XSV(21)
      COMMON /EPSIL/EPSETA,EPST,EPSR
      COMMON /EXTREM/TEXT(5),ETAEXT(5),ETAKXT(5),PHIEXT(5),
     1             PSIEXT(5),EMEXT(5),FEXT(5),WEXT(5),
     2             TMAX(5),ETAKMX(5),ETAMAX(5),PSIMAX(5),
     3             EMMAX(5),FMAX(5),
     4             RFMAX(5),PHIFMX(5),PHIMAX(5),WMAX(5)
      COMMON /COUNTS/ICONTC,ICONTT,ICNTOT,ICNTMX,IQTOT(5),ISHAD(5)
```

```
      COMMON /AMBIEN/ENA,UA,PSIA,PHIA,HA(3),WA(3),
     1               UAX,UAY,UAZ,AA,BA,CA,RA,XA,YA,ZA,SHADOW
      LOGICAL SHADOW
      ETAK=0.
C  DETERMINE POINT OF ENTRY OF AMBIENT TRAJECTORY TO FAN
      TRF=T*RF
      XC=XF+TRF*OMEGX
      YC=YF+TRF*OMEGY
      ZC=ZF+TRF*OMEGZ
C  CHECK SHADOW
      SHADOW=.FALSE.
      EVER=BA**2+CA**2
      DETS=EVER*A0**2-(BA*ZC-CA*YC)**2
      IF(DETS.LE.0.) GO TO 2
      DETS1=DSQRT(DETS)
      TAU1=(-(BA*YC+CA*ZC)+DETS1)/EVER
      IF(TAU1.GT.0.) SHADOW=.TRUE.
 2    CONTINUE
      IF(SHADOW) GO TO 10
      EVER1=A0+XC*TPSIF
      EVER2=BA**2+CA**2-(AA*TPSIF)**2
      EVER3=BA*YC+CA*ZC-AA*EVER1*TPSIF
      DET=EVER3**2-EVER2*(YC**2+ZC**2-EVER1**2)
      IF(DET.LE.0.)
     1CALL SOF('NO INTERSECTION OF AMB. TRAJ. WITH LIMITING CONE')
      DET1=DSQRT(DET)
      TAUP=(-EVER3+DET1)/EVER2
      TAUM=(-EVER3-DET1)/EVER2
      IF(TAUP.GT.0. .AND. TAUM.GT.0.)
     1CALL SOF('TWO POSITIVE INTERSECTIONS WITH LIMITING CONE.NOT PERMIT
     1 IN THIS VERSION')
      TAUF=DMAX1(TAUP,TAUM)
      IF(TAUF.LE.0.)
     1CALL SOF('NO POSITIVE INTERSECTION WITH LIMITING CONE')
      XA=XC+TAUF*AA
      YA=YC+TAUF*BA
      ZA=ZC+TAUF*CA
      RA=DSQRT(XA**2+(DSQRT(YA**2+ZA**2)-A0)**2)
      TAUF=TAUF/RA
      NTAU=NTAU0
      DTAU=TAUF/DBLE(NTAU)
      ETAK=0.
      TAU=0.
      DTAU2=DTAU/2.D0
      DTAU6=DTAU/6.D0
      GTAU4=0.
      ITAU=0
 1    ITAU=ITAU+1
      TAU1=TAU+DTAU2
      TAU2=TAU+DTAU
      GTAU1=GTAU4
      CALL FTAU(TAU1,GTAU2)
      GTAU3=GTAU2
      CALL FTAU(TAU2,GTAU4)
      DETAK=DTAU6*(GTAU1+2.D0*(GTAU2+GTAU3)+GTAU4)
      TAU=TAU+DTAU
      ETAK=ETAK+DETAK
      IF(ITAU.LT.NTAU) GO TO 1
      ETAK=ETAK*(SIGMA*EN0*RA)
      RETURN
 10   CONTINUE
      ISHAD(NS)=ISHAD(NS)+1
      RETURN
      END
      SUBROUTINE FTAU(TAU,GTAU)
      IMPLICIT REAL*8(A-H,O-Z)
      COMMON /GAMA/G,G1,G2,G3,G4,G5,G6,G7,G8,G9,G10,G11,G12,G13,G14,G15,
     1             G16,G17,G18,G19,G20
      COMMON /PAR/C0,EN0,EM1,D,SIGMA,TLIM,DR0,EL0,Q0,T0,FACT,ALOGF,
     1            DPSI0,DTMAX,DETA0,ETALIM,XSI,XSF
      COMMON /NPAR/NPHI,IPAR,NP,NR,NX,NXS,NS,NSPEC,NS1,NS2,NTAU0,NETA0,
     1             NAMB,NCASE,ICASE,IFAN
```

```
      COMMON /GEOM/APF,PAI,PAI2,W,SW,CW,BETA,SBETA,CBETA,PSI1,SPSI1,
     1          CPSI1,PSIF,SPSIF,CPSIF,TPSIF,AK,SK,CK,A0,RF,XF,YF,ZF,
     2          PHISOF,PHIF,SPHIF,CPHIF,DYMIN,RMIN,XS,DIST,X0,Y0,Z0,
     3          DY0,DEG,PSIN,ST1,CT1,OMEGX,OMEGY,OMEGZ,XSV(21)
      COMMON /EPSIL/EPSETA,EPST,EPSR
      COMMON /EXTREM/TEXT(5),ETAEXT(5),ETAKXT(5),PHIEXT(5),
     1            PSIEXT(5),EMEXT(5),FEXT(5),WEXT(5),
     2            TMAX(5),ETAKMX(5),ETAMAX(5),PSIMAX(5),
     3            EMMAX(5),FMAX(5),
     4            RFMAX(5),PHIFMX(5),PHIMAX(5),WMAX(5)
      COMMON /SPEC/WAV,XC(5),WC(5),WRC(5),XNAME(5),QFC(5),QDC(5),
     1          QU2C(5),FLUXC(5),OMEGA(5),FLXU2C(5),URMSC(5)
      COMMON /AMBIEN/ENA,UA,PSIA,PHIA,HA(3),WA(3),
     1            UAX,UAY,UAZ,AA,BA,CA,RA,XA,YA,ZA,SHADOW
      LOGICAL SHADOW
      CALL FANT(TAU,PSI,PHI)
      IF(PSI.LT.PSIF-1.D-10) CALL SOF('PSI.LT.PSIF')
      IF(PSI.GT.PSI1) PSI=PSI1
      PSI0=PSI
      CALL MATCH(T,PSI0,EM,TETA)
      SPSI=DSIN(PSI)
      CPSI=DCOS(PSI)
      SPHI=DSIN(PHI)
      CPHI=DCOS(PHI)
      ST=DSIN(TETA)
      CT=DCOS(TETA)
      GOREM=1.D0+G1*EM**2
      TERMN=GOREM**G6
      U=EM*C0/DSQRT(GOREM)
      UREL=DSQRT((CT*U-UAX)**2+(ST*CPHI*U-UAY)**2+(ST*SPHI*U-UAZ)**2)
      GTAU=UREL/(UA*TERMN)
      RETURN
      END
      SUBROUTINE FAN(T,PSI,PHI)
      IMPLICIT REAL*8(A-H,O-Z)
      COMMON /PAR/C0,EN0,EM1,D,SIGMA,TLIM,DR0,EL0,Q0,T0,FACT,ALOGF,
     1         DPSI0,DTMAX,DETA0,ETALIM,XSI,XSF
      COMMON /GEOM/APF,PAI,PAI2,W,SW,CW,BETA,SBETA,CBETA,PSI1,SPSI1,
     1          CPSI1,PSIF,SPSIF,CPSIF,TPSIF,AK,SK,CK,A0,RF,XF,YF,ZF,
     2          PHISOF,PHIF,SPHIF,CPHIF,DYMIN,RMIN,XS,DIST,X0,Y0,Z0,
     3          DY0,DEG,PSIN,ST1,CT1,OMEGX,OMEGY,OMEGZ,XSV(21)
      COMMON /POINT/XP,YP,XCOR,YCOR
C  RING FAN GEOMETRY.   FAN CORNER IS AT (0,A0*COS(PHI),A0*SIN(PHI)).
C  RF  --  RADIAL DISTANCE ON LIMITING CHARACTERISTIC OF POINT OF
C          ENTRANCE OF RAY.
C  DIRECTION COSINES OF RAY: OMEGX,OMEGY,OMEGZ
      TRF=T*RF
      X=XF+TRF*OMEGX
      Y=YF+TRF*OMEGY
      Z=ZF+TRF*OMEGZ
      DY=DSQRT(Y*Y+Z*Z)-A0
      IF(DABS(DY).LE.1.D-10*A0) DY=1.D-10*A0
      IF(DY.LT.0.)
     1CALL SOF('POINT X,Y,X CANNOT BE CLOSER TO X-AXIS THAN RADIUS A0')
      YY=X/DY
      PSI=PAI2-DATAN(YY)
      PHI=DATAN(Z/Y)
      XP=XCOR+X
      YP=A0+DY
      RETURN
      END
      SUBROUTINE FANT(TAU,PSI,PHI)
      IMPLICIT REAL*8(A-H,O-Z)
      COMMON /PAR/C0,EN0,EM1,D,SIGMA,TLIM,DR0,EL0,Q0,T0,FACT,ALOGF,
     1         DPSI0,DTMAX,DETA0,ETALIM,XSI,XSF
      COMMON /GEOM/APF,PAI,PAI2,W,SW,CW,BETA,SBETA,CBETA,PSI1,SPSI1,
     1          CPSI1,PSIF,SPSIF,CPSIF,TPSIF,AK,SK,CK,A0,RF,XF,YF,ZF,
     2          PHISOF,PHIF,SPHIF,CPHIF,DYMIN,RMIN,XS,DIST,X0,Y0,Z0,
     3          DY0,DEG,PSIN,ST1,CT1,OMEGX,OMEGY,OMEGZ,XSV(21)
      COMMON /AMBIEN/ENA,UA,PSIA,PHIA,HA(3),WA(3),
     1            UAX,UAY,UAZ,AA,BA,CA,RA,XA,YA,ZA,SHADOW
      COMMON /POINT/XP,YP,XCOR,YCOR
```

```
      LOGICAL SHADOW
C  RING FAN GEOMETRY.   FAN CORNER IS AT (0,A0*COS(PHI),A0*SIN(PHI)).
C  RA  --   RADIAL DISTANCE ON LIMITING CHARACTERISTIC OF POINT OF
C              ENTRANCE OF RAY.
C  DIRECTION COSINES OF RAY: -AA,-BA,-CA
      TRA=TAU*RA
      X=XA-TRA*AA
      Y=YA-TRA*BA
      Z=ZA-TRA*CA
      DY=DSQRT(Y*Y+Z*Z)-A0
      IF(DABS(DY).LE.1.D-10*A0) DY=1.D-10*A0
      IF(DY.LT.0.)
     1CALL SOF('POINT X,Y,X CANNOT BE CLOSER TO X-AXIS THAN RADIUS A0')
      YY=X/DY
      PSI=PAI2-DATAN(YY)
      PHI=DATAN(Z/Y)
      XP=XCOR+X
      YP=A0+DY
      RETURN
      END
      SUBROUTINE HMSET
C  SUBROUTINE NUMBER  20
      IMPLICIT REAL*8(A-H,O-Z,$)
      REAL*8 KAPA0B,MHINV,MINV0,M,MF,M1,M2,M3,NORM,MEXIT,LAMD0B
      COMMON /GAMA/G,G1,G2,G3,G4,G5,G6,G7,G8,G9,G10,G11,G12,G13,G14,G15,
     1                 G16,G17,G18,G19,G20
      COMMON /PAR/C0,EN0,EM1,D,SIGMA,TLIM,DR0,EL0,Q0,T0,FACT,ALOGF,
     1               DPSI0,DTMAX,DETA0,ETALIM,XSI,XSF
      COMMON /GEOM/APF,PAI,PAI2,W,SW,CW,BETA,SBETA,CBETA,PSI1,SPSI1,
     1                 CPSI1,PSIF,SPSIF,CPSIF,TPSIF,AK,SK,CK,A0,RF,XF,YF,ZF,
     2                 PHISOF,PHIF,SPHIF,CPHIF,DYMIN,RMIN,XS,DIST,X0,Y0,Z0,
     3                 DY0,DEG,PSIN,ST1,CT1,OMEGX,OMEGY,OMEGZ,XSV(21)
      COMMON /GRP/DMINV,MHINV(101),HMV(101)
      COMMON /IGRP/KHM
C  A ROUTINE FOR THE C+ DERIVATIVE DUE TO RING SYMMETRY (GRP).
      MEXIT=EM1
      KHM=51
      IF(KHM.GT.101) CALL SOF('2001')
      MINV0=1.D0/MEXIT
      DMINV=MINV0/DBLE(KHM-1)
      M=MEXIT
      SUM=0.
      KHM1=KHM-1
      DO 1 I=1,KHM1
      MF=M
      MHINV(I)=MINV0-DBLE(I-1)*DMINV
      M=1.D0/MHINV(I)
      DM=M-MF
      M1=M-DM
      M2=M-DM/2.D0
      M3=M
      CALL MFUNC(M1,F1,ETALF1,TETA1)
      CALL MFUNC(M2,F2,ETALF2,TETA2)
      CALL MFUNC(M3,F3,ETALF3,TETA3)
      SUM=SUM+DM*(F1+4.D0*F2+F3)/6.D0
      ETALF=ETALF3
      TETA=TETA3
      PSI=TETA+DASIN(1.D0/M)
      NORM=((3.D0-G)/4.D0)*(M**2-1.D0)**0.75D0/
     1      (DSIN(PSI)*(1.D0+G1*M**2)**G14)
      HM=SUM*NORM
      HMV(I)=HM
      GOREM=1.D0+G1*M**2
      GOR=M**2-1.D0
      DELT0B=0.5D0*DSQRT(GOR)*(1.D0/(MEXIT*ETALF)
     1       +DSIN(TETA)/M)/DSIN(PSI)+G15*HM/2.D0
      EPSI0B=DELT0B/DSQRT(GOR)-DSIN(TETA)/(M*DSIN(PSI))
      KAPA0B=1.D0
      IF(DABS(PAI2-TETA).GT.1.D-6)
     1KAPA0B=DTAN(TETA)*EPSI0B
      LAMD0B=EPSI0B-DELT0B*GOREM/(GOR*DSQRT(GOR))
      PRINT 11,I,M,HM,TETA*DEG,PSI*DEG
```

```
 11    FORMAT(/1X,'              I,M,HM,TETA,PSI=',I5,5D12.4)          AMB1081
       PRINT 12,DELTOB,EPSIOB*DEG,KAPAOB*DEG,LAMDOB*DEG                AMB1082
 12    FORMAT( 1X,'DELTOB,EPSIOB,KAPAOB,LAMDOB=',5X,5D12.4)            AMB1083
 1     CONTINUE                                                        AMB1084
       MHINV(KHM)=0.                                                   AMB1085
       HMV(KHM)=1.D0                                                   AMB1086
       RETURN                                                          AMB1087
       END                                                             AMB1088
       SUBROUTINE MFUNC(M,F,ETALF,TETA)                                AMB1089
C  SUBROUTINE NUMBER  21                                               AMB1090
       IMPLICIT REAL*8(A-H,O-Z,$)                                      AMB1091
       REAL*8 NU,NUFUNC,M,MEXIT,MD,MDD                                 AMB1092
       COMMON /GAMA/G,G1,G2,G3,G4,G5,G6,G7,G8,G9,G10,G11,G12,G13,G14,G15,AMB1093
     1             G16,G17,G18,G19,G20                                 AMB1094
       COMMON /PAR/C0,EN0,EM1,D,SIGMA,TLIM,DR0,EL0,Q0,T0,FACT,ALOGF,   AMB1095
     1            DPSI0,DTMAX,DETA0,ETALIM,XSI,XSF                     AMB1096
       COMMON /GEOM/APF,PAI,PAI2,W,SW,CW,BETA,SBETA,CBETA,PSI1,SPSI1,  AMB1097
     1             CPSI1,PSIF,SPSIF,CPSIF,TPSIF,AK,SK,CK,A0,RF,XF,YF,ZF,AMB1098
     2             PHISOF,PHIF,SPHIF,CPHIF,DYMIN,RMIN,XS,DIST,X0,Y0,Z0, AMB1099
     3             DY0,DEG,PSIN,ST1,CT1,OMEGX,OMEGY,OMEGZ,XSV(21)      AMB1100
C                                                                      AMB1101
       QF(MDD)=1.D0/DSQRT(MDD**2-1.D0)                                 AMB1102
       NUFUNC(MD)=-G5*DATAN(G5*QF(MD))+DATAN(QF(MD))                   AMB1103
C                                                                      AMB1104
       MEXIT=EM1                                                       AMB1105
       NU=NUFUNC(M)                                                    AMB1106
       TETA=NUFUNC(MEXIT)+PAI2-NU                                      AMB1107
       GOREM=1.D0+G1*M**2                                              AMB1108
       GOR=M**2-1.D0                                                   AMB1109
       F=(M**2)*(GOREM**G13)*DSIN(TETA)/GOR**1.25D0                    AMB1110
       GOREM1=1.D0+G1*MEXIT**2                                         AMB1111
       GOR1=MEXIT**2-1.D0                                              AMB1112
       ETALF=((GOREM/GOREM1)**G14)*((GOR1/GOR)**0.25D0)                AMB1113
       RETURN                                                          AMB1114
       END                                                             AMB1115
       SUBROUTINE HINTER(M,H)                                          AMB1116
C  SUBROUTINE NUMBER  22                                               AMB1117
       IMPLICIT REAL*8(A-H,O-Z,$)                                      AMB1118
       REAL*8 MINV,M,MEXIT,MHINV                                       AMB1119
       COMMON /GAMA/G,G1,G2,G3,G4,G5,G6,G7,G8,G9,G10,G11,G12,G13,G14,G15,AMB1120
     1             G16,G17,G18,G19,G20                                 AMB1121
       COMMON /PAR/C0,EN0,EM1,D,SIGMA,TLIM,DR0,EL0,Q0,T0,FACT,ALOGF,   AMB1122
     1            DPSI0,DTMAX,DETA0,ETALIM,XSI,XSF                     AMB1123
       COMMON /GRP/DMINV,MHINV(101),HMV(101)                           AMB1124
       COMMON /IGRP/KHM                                                AMB1125
C COMPUTE H(M) BY INTERPOLATION                                        AMB1126
       MEXIT=EM1                                                       AMB1127
       MINV=1.D0/M                                                     AMB1128
       I=KHM-IDINT(MINV/DMINV-1.D-9)-1                                 AMB1129
       IF(I.GE.1.AND.I.LT.KHM) GO TO 1                                 AMB1130
       PRINT 11,I,KHM,M,MEXIT                                          AMB1131
 11    FORMAT(/1X,'I,KHM,M,MEXIT=',2I5,2D14.6/)                        AMB1132
       CALL SOF('2201')                                                AMB1133
 1     CONTINUE                                                        AMB1134
       F1=(MINV-MHINV(I+1))/DMINV                                      AMB1135
       F2=1.D0-F1                                                      AMB1136
       IF(F1.LT.-1.D-9) CALL SOF('2210')                               AMB1137
       IF(F2.LT.-1.D-9) CALL SOF('2211')                               AMB1138
       H=F1*HMV(I)+F2*HMV(I+1)                                         AMB1139
       RETURN                                                          AMB1140
       END                                                             AMB1141
       SUBROUTINE MATCH(T,PSI0,MAB,TETAAB)                             AMB1142
C  SUBROUTINE NUMBER  23                                               AMB1143
       IMPLICIT REAL*8(A-H,O-Z,$)                                      AMB1144
       REAL*8 M,MOB,MEXIT,MAB,LAMDOB,KAPAOB                            AMB1145
       COMMON /GAMA/G,G1,G2,G3,G4,G5,G6,G7,G8,G9,G10,G11,G12,G13,G14,G15,AMB1146
     1             G16,G17,G18,G19,G20                                 AMB1147
       COMMON /PAR/C0,EN0,EM1,D,SIGMA,TLIM,DR0,EL0,Q0,T0,FACT,ALOGF,   AMB1148
     1            DPSI0,DTMAX,DETA0,ETALIM,XSI,XSF                     AMB1149
       COMMON /NPAR/NPHI,IPAR,NP,NR,NX,NXS,NS,NSPEC,NS1,NS2,NTAU0,NETA0, AMB1150
     1             NAMB,NCASE,ICASE,IFAN                               AMB1151
       COMMON /GEOM/APF,PAI,PAI2,W,SW,CW,BETA,SBETA,CBETA,PSI1,SPSI1,  AMB1152
```

```
     1              CPSI1,PSIF,SPSIF,CPSIF,TPSIF,AK,SK,CK,A0,RF,XF,YF,ZF,
     2              PHISOF,PHIF,SPHIF,CPHIF,DYMIN,RMIN,XS,DIST,X0,Y0,Z0,
     3              DY0,DEG,PSIN,ST1,CT1,OMEGX,OMEGY,OMEGZ,XSV(21)
      COMMON /POINT/XP,YP,XCOR,YCOR
      COMMON /GRP/DMINV,MHINV(101),HMV(101)
      COMMON /IGRP/KHM
      MEXIT=EM1
      GO TO (101,102),IFAN
  101 CONTINUE
C  FAN APPROXIMATED AS PLANAR
      MAB=DSQRT(1.D0+G4/DTAN((PSI0-PSIF)/G5)**2)
      TETAAB=PSI0-DASIN(1.D0/MAB)
      GO TO 100
  102 CONTINUE
C  COMPUTE MAB FROM THE INVERSE PROBLEM SOLUTION
      COTAV=1.D0/DTAN(PSI0)
      EVY=YP*DLOG(YP/YCOR)/(YP-YCOR)-1.D0
      PSIN=PSI0
      DO 1 ITER=1,10
      PSI=PSIN
      M=DSQRT(1.D0+G4/DTAN((PSI-PSIF)/G5)**2)
      M=DMAX1(M,MEXIT)
      CALL HINTER(M,HM)
      CALL MFUNC(M,F,ETALF,TETA)
      GOREM=1.D0+G1*M**2
      GOR=M**2-1.D0
      DELTOB=0.5D0*DSQRT(GOR)*(1.D0/(MEXIT*ETALF)
     1        +DSIN(TETA)/M)/DSIN(PSI)+G15*HM/2.D0
      EPSIOB=DELTOB/DSQRT(GOR)-DSIN(TETA)/(M*DSIN(PSI))
      LAMDOB=EPSIOB-DELTOB*GOREM/(GOR*DSQRT(GOR))
      COTN=COTAV+LAMDOB*EVY/DSIN(PSI)**2
      PSIN=PAI2-DATAN(COTN)
      DPSI=PSIN-PSI
      IF(DABS(DPSI).LT.1.D-6) GO TO 11
    1 CONTINUE
      PRINT 12,I,ITER,PSI,PSIN,DPSI,M,XP,YP,T
   12 FORMAT(/1X,'I,ITER,PSI,PSIN,DPSI,M,XP,YP,T='//
     1        1X,2I4,7D11.3/)
      CALL SOF('2301')
   11 CONTINUE
C  USING MOB=M AS COMPUTED FROM THE INVERSE PROBLEM, FIND MAB.
      MOB=M
      CALL MFUNC(M,F,ETALF,TETA)
      PSI=TETA+DASIN(1.D0/M)
      CALL HINTER(M,HM)
      GOREM=1.D0+G1*M**2
      GOR=M**2-1.D0
      DELTOB=0.5D0*DSQRT(GOR)*(1.D0/(MEXIT*ETALF)
     1       +DSIN(TETA)/M)/DSIN(PSI)+G15*HM/2.D0
      FOB=(G7*GOREM)**G2/M
      FAB=FOB*(YP/YCOR)**DELTOB
      CALL AREAF(FAB,MAB)
      EPSIOB=DELTOB/DSQRT(GOR)-DSIN(TETA)/(M*DSIN(PSI))
      KAPAOB=1.D0
      IF(DABS(PAI2-TETA).GT.1.D-8)
     1KAPAOB=DTAN(TETA)*EPSIOB
      COSTAB=DCOS(TETA)*(YP/YCOR)**(-KAPAOB)
      TETAAB=DACOS(COSTAB)
  100 CONTINUE
      RETURN
      END
      SUBROUTINE AREAF(F,M)
C  SUBROUTINE NUMBER  24
      IMPLICIT REAL*8(A-H,O-Z,$)
      REAL*8 MEXIT,MIN,M,MHINV
      COMMON /GAMA/G,G1,G2,G3,G4,G5,G6,G7,G8,G9,G10,G11,G12,G13,G14,G15,
     1              G16,G17,G18,G19,G20
      COMMON /PAR/C0,EN0,EM1,D,SIGMA,TLIM,DR0,EL0,Q0,T0,FACT,ALOGF,
     1             DPSI0,DTMAX,DETA0,ETALIM,XSI,XSF
      COMMON /GRP/DMINV,MHINV(101),HMV(101)
      COMMON /IGRP/KHM
C  COMPUTE MACH NUMBER M FROM AREA RATIO FUNCTION F
```

```
C  F=((2/(G+1))*(1+(G-1)*M**2))**((G+1)/(2*(G-1)))/M
C  INITIAL GUESS IS MIN
      MEXIT=EM1
      E1=(F*MEXIT)**(1.D0/G2)/G7
      E2=(E1-1.D0)/G1
      E3=DMAX1(E2,MEXIT**2)
      MIN=DSQRT(E3)
      EMN=MIN
      DO 1 I=1,100
      EMO=EMN
      GOREM=1.D0+G1*EMO**2
      GOR=EMO**2-1.D0
      FO=(C7*GOREM)**G2/EMO
      DF=FO-F
C     PRINT 123,I,EMO,EMN,FO,F,DF,GOR,GOREM
C123  FORMAT(1X,'I,EMO,EMN,FO,F,DF,GOR,GOREM=',I5,7D12.4)
      DFDM=FO*GOR/(EMO*GOREM)
      DMN=DF/DFDM
      EMN=EMO-DMN
      EPSEM=DABS(DMN/EMN)
      IF(EPSEM.LT.1.D-10) GO TO 11
 1    CONTINUE
      CALL SOF('2401')
 11   CONTINUE
      M=EMN
      RETURN
      END
```

## 8. DISTRIBUTION LIST

No. of Copies

1. Defense Technical Information Center
Cameron Station
Alexandria, VA 22314 . . . . . . . . . . . . . . . . . . . . . . . . 2

2. Library, Code 0142
Naval Postgraduate School
Monterey, CA 93943-5100. . . . . . . . . . . . . . . . . . . . . . . 2

3. Department Chairman, Code 67
Department of Aeronautics
Naval Postgraduate School
Monterey, CA 93943-5100. . . . . . . . . . . . . . . . . . . . . . . 1

4. Distinguished Professor Allen E. Fuhs
Space Systems Academic Group, Code 72
Naval Postgraduate School
Monterey, CA 93943-5100. . . . . . . . . . . . . . . . . . . . . . . 5

5. Dr. Neil Griff
SDIO DEO
Washington, DC 20301-7100. . . . . . . . . . . . . . . . . . . . . . 3

6. Mr. Bruce Pierce
SDIO DEO
Washington, DC 20301-7100. . . . . . . . . . . . . . . . . . . . . . 1

7. Dr. Joseph Falcovitz (24)
Rafael Ballistic Center
P. O. Box 2250, Haifa
Israel . . . . . . . . . . . . . . . . . . . . . . . . . . . . . . . 5

No. of Copies

8. Professor Oscar Biblarz
Department of Aeronautics, Code 67
Naval Postgraduate School
Monterey, CA 93943-5100. . . . . . . . . . . . . . . . . . . . . . 1

9. Research Administration Office
Code 012
Naval Postgraduate School
Monterey, CA 93943-5100. . . . . . . . . . . . . . . . . . . . . . 1

10. Dr. P. Avizonis
Air Force Weapons Laboratory
Kirtland Air Force Base, NM 87117 . . . . . . . . . . . . . . . . . . 1

11. Dr. John Lawless
Space Power Inc.
1977 Concourse Drive
San Jose, CA 95131 . . . . . . . . . . . . . . . . . . . . . . . . 1

12. Dr. Mark Thornton
Boeing Aerospace Company
Post Office Box 3999
Seattle, WA 98124-2499 . . . . . . . . . . . . . . . . . . . . . . 1

13. LT. Mark Price
AFRPL
Edwards AFB, CA 93523 . . . . . . . . . . . . . . . . . . . . . . 1

14. Mr. Arthur W. Rogers
Space Systems Division
Hughes Aircraft Co.
P. O. Box 92919, Los Angeles, CA 90009 . . . . . . . . . . . . . . . 1

No. of Copies

15. LCOL Rick Babcock, USAF
Air Force Geophysical Laboratory
Hanscomb Field
Bedford, MA 01730 . . . . . . . . . . . . . . . . . . . . . . . . 1

16. Mr. Ronald J. Hoffman
Plume Technology and Spacecraft
Contamination Division
Science Applications International Co.
10000 Santa Monica Blvd., Suite 320
Los Angeles, CA 90067 . . . . . . . . . . . . . . . . . . . . . . . 1

END
9-87
DTIC